GERMANIUM LITHIUM-DRIFTED

DETECTORS

COAXIAL
GERMANIUM LITHIUM-DRIFTED
GAMMA RADIATION DETECTORS

By

BASIL JOHN WALL, B.Sc.

A Thesis

Submitted to the Faculty of Graduate Studies

in Partial Fulfilment of the Requirements

for the Degree

Master of Science

McMaster University

September, 1966

MASTER OF SCIENCE (1966) McMASTER UNIVERSITY
Hamilton, Ontario

TITLE: Coaxial Germanium Lithium-Drifted Gamma Radiation Detectors

AUTHOR: Basil John Wall, B.Sc. (McMaster University)

SUPERVISOR: Dr. T. J. Kennett

NUMBER OF PAGES: vi, 56

SCOPE AND CONTENTS:

This thesis deals with the theory, fabrication and application of semi-conductor detectors to gamma ray spectroscopy. The theory section discusses the semi-conductor lattice with respect to the incoming gamma ray and the subsequent hole-electron pairs formed in the diode depletion region. The fabrication section describes the materials and apparatus used in this work to produce the Ge(Li) detectors. A table is given showing the characteristics of these devices as they proceed through the process. The section on the characteristics of these detectors gives information as to how a good detector should operate under certain tests.

The detectors made in this laboratory were used to investigate a well known "fission product" nuclide and a neutron capture reaction on a rare earth element. However, these investigations were not exhaustive but only show how the improved resolution of the Ge(Li) detectors has opened up new areas of gamma ray studies.

ACKNOWLEDGEMENTS

I wish to express appreciation to my Research Director, Dr. T. J. Kennett for his encouragement and advice throughout this work. I also wish to thank all those who were involved in any way with this research for their assistance both practical and impractical. Appreciation also goes to Mrs. H. Kennelly who typed this thesis and did a very fine piece of work.

TABLE OF CONTENTS

LIST OF TABLES

LIST OF ILLUSTRATIONS

CHAPTER I

INTRODUCTION

With the introduction of the ion drift technique by Pell[15] in 1960 and its improvement by Miller et al[16], a new type of gamma radiation detector made its appearance. The initial devices consisted of p-n silicon semiconductor diodes in a planar type configuration with up to 10 mm depletion depth. Planar germanium lithium drifted devices were also introduced and because of the higher atomic number of germanium, the reaction cross section for gamma ray interaction increased over that for the silicon devices. The next step in the development of efficient high resolution detectors was the fabrication of co-axial type Ge(Li) detectors in which lithium is evaporated onto five sides of a germanium crystal and then alloyed into the semiconductor[7]. A specific diode reported in reference (7) had an active volume of 16 c.c. and was used as a high resolution spectrometer by Malm et al[3] in 1965. The advantage of the co-axial configuration over the planar type of detectors is that a much larger active volume can be achieved in the former than the latter for the same period of drift. These larger volumes are at present being used in coincidence experiments because of their increased efficiency and resolution. One example of a coincidence type experiment is given in the final chapter of this thesis.

Some of the research reported in this thesis was submitted for publication in 1965[5] at which time a 6 c.c. and a 10 c.c. detector were in operation in this laboratory as spectrometers. In this laboratory a new technique was established for depositing lithium onto p-type germanium. This

involves electroplating the lithium from a lithium salt solution on the five sides of the crystal and simultaneously alloying this lithium to the germanium at elevated temperatures. Most other experimenters reporting to date use a two step process whereby they first evaporate lithium onto the crystal and then heat the crystal and lithium to achieve the thin alloyed layer. Many other advances have been made in the last year. Tavendale[3] has reported active volume of 54 c.c and greatly improved resolution using field effect transistors in the pre-amplifying system. Surface treatments have been investigated by Armantrout[4] and also in this work. A comprehensive report on recent advances is presented in reference (17).

CHAPTER II

THEORY OF GAMMA RADIATION DETECTORS

2.1 Introduction

Gamma radiation detectors for energy measurements in past years have been of two basic designs; these are based upon the properties of ionization of gas and the scintillation associated with organic or inorganic crystals. As the ions are formed in the discharge type ($\sim$ 33 eV per ion pair) a high electric field ($\sim$1,000 volts/cm) sweeps these charge carriers through the detection system and since the number of ions created is proportional to the energy absorbed in the detector, the pulse can be analyzed in a multi-channel analyzer.

The operating principle of scintillation detectors depends on the light emitted by the interaction of the gamma rays with the atoms of the scintillating material, usually sodium iodide activated with thallium. The intensity of the light emitted is proportional to the energy absorbed in the scintillator, and this light is converted via a photo multiplier tube into an electrical pulse which is analyzed. The energy resolution of these detectors ($\sim$ 8% for a NaI(Tℓ) device) was not adequate for many energy measurements, thus new devices with better resolution were sought.

By 1960 a new type of discharge detector was introduced. Basically the device consists of a semi-conductor diode, which can be fabricated with almost any intrinsic volume desired, up to ~ 60 cm^3.

This diode when reverse biased can produce a high electric field in the large volume of the depletion region. Thus when gamma rays interact by the photo electric effect, the Compton effect or the pair producing effect, which result in the production of hole-electron pairs, the energy proportional pulse can be analyzed. Figure (1) gives a comparison of a sodium iodide spectrum with a Ge(Li) spectrum of the same radioactive source. The improvement in resolution of the germanium Ge(Li) detectors over the sodium iodide detectors is dramatically obvious. The principle of this device is similar to an ionization chamber but has a higher density and a lower ionization energy than the gaseous counterpart.

2.2 The Semi-Conductor Diode

Consider the junction between p-type, gallium doped, germanium (40Ω-cms) and n-type , lithium alloyed, germanium with sheet resistivity of 0.01$\Omega/\square$. In the p-type semi-conductor the charge carriers are predominantly holes, while in the n-type material the carriers are electrons. Therefore at the junction there will be a diffusion of these carriers across their respective concentration gradients. As this diffusion takes place, the region of the junction builds up a voltage which prevents the further diffusion of carriers as shown in Figure (2). The diagram which depicts the same situation as derived from the Band Theory is shown in Figure (3a), where E_c is the energy of the conduction band, E_v is the valence band energy and E_F is the Fermi level energy. This is the energy scheme for electrons. For holes, the bands are reflected in the junction plane and all the signs of charges are reversed. To use the diode as a counter with the high field in the depletion region, a reverse bias is applied as shown in Figure (3b). However for an efficient counter the depletion depth X must be a few millimeters. The

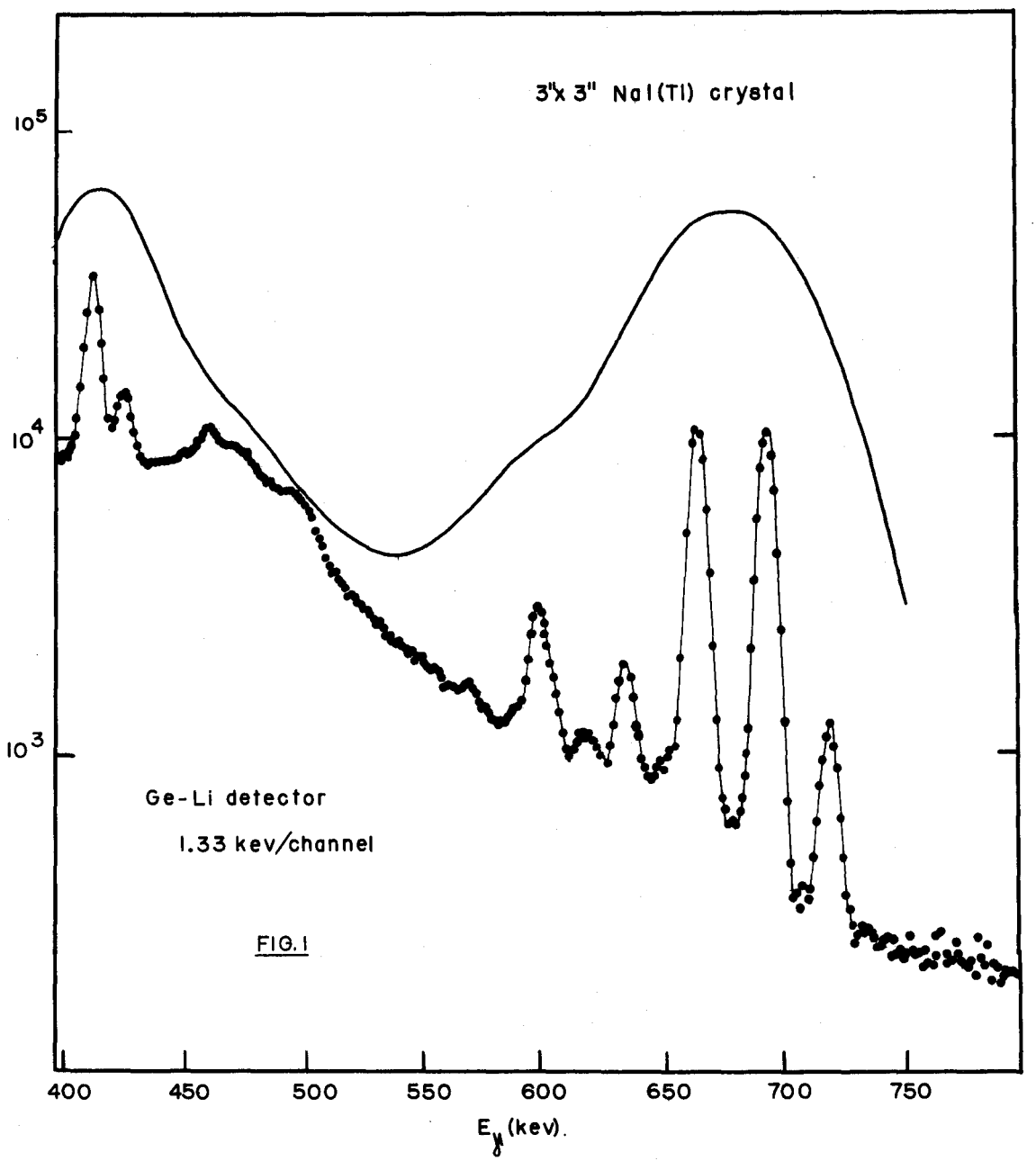
3"x 3" NaI(Tl) crystal
10^5
10^4
10^3
Ge-Li detector
1.33 kev/channel
400
450
500
550
600
650
700
750
E_γ (kev).

FIG. 1

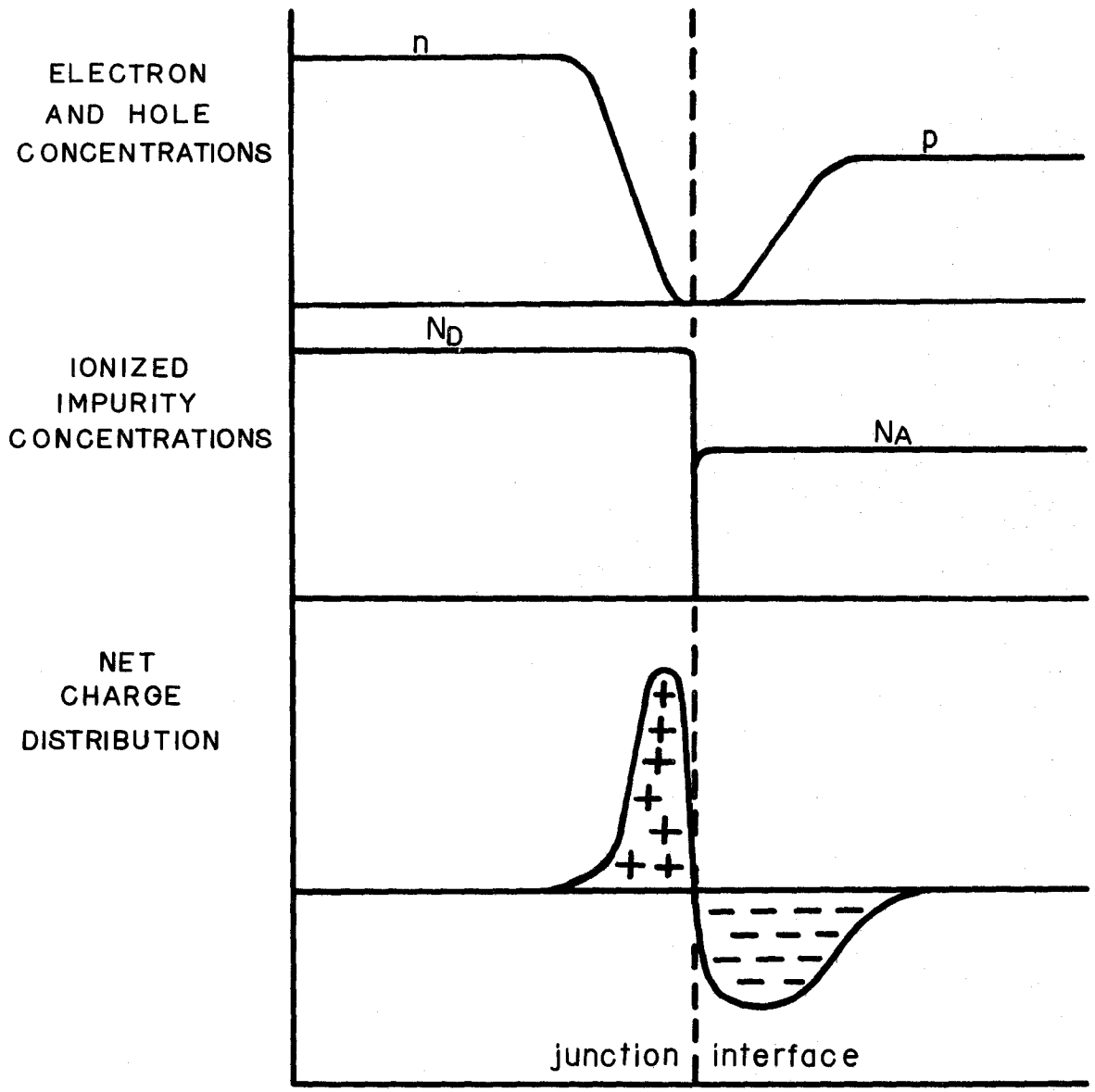

P-N JUNCTION

FIG. 2

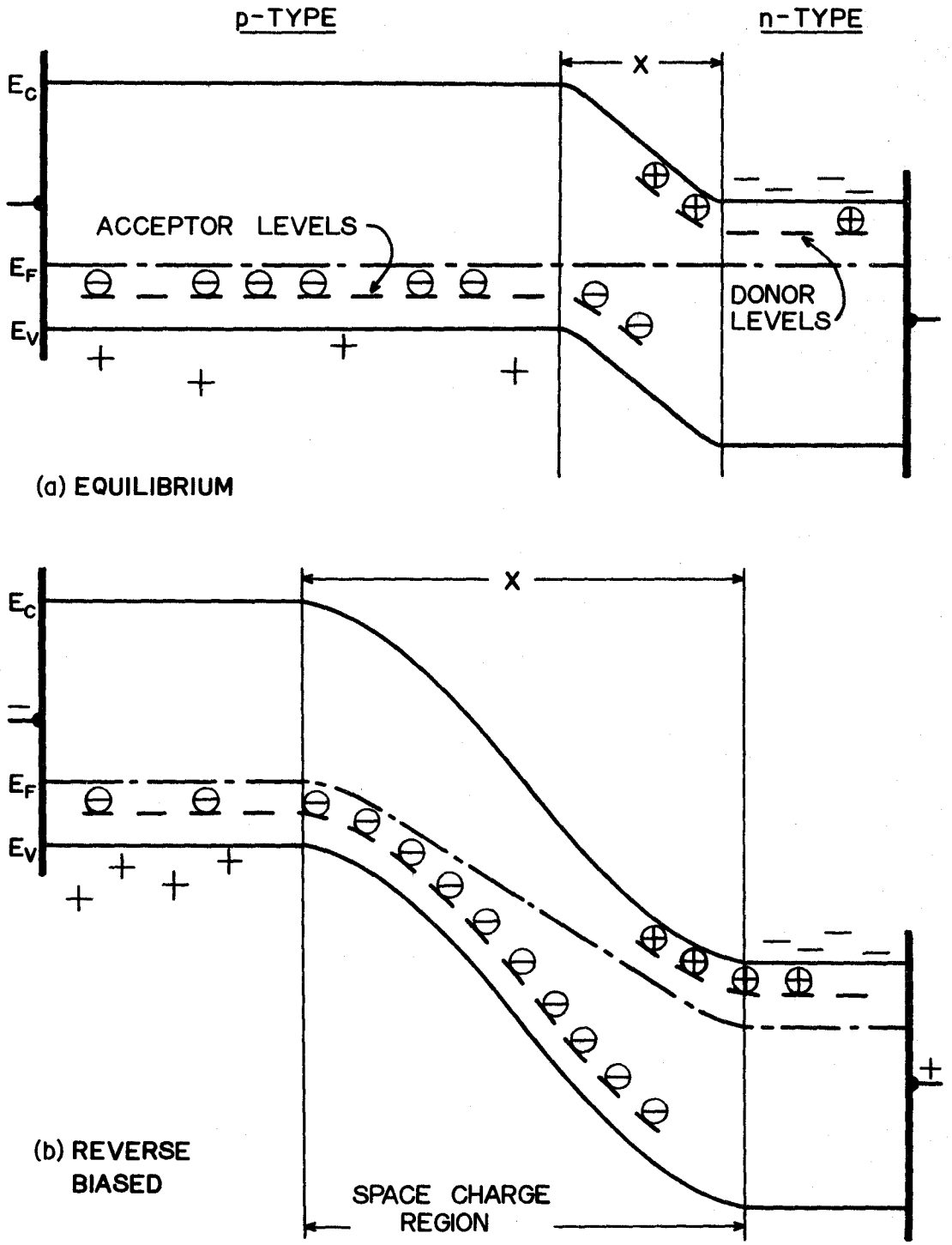

BAND SCHEME FOR A p-n JUNCTION

FIG.3

"wrap-around" or co-axial configuration of the detectors investigated in this thesis have n-type semi-conductor on five sides of an ingot and a p-type core as shown in Figure (4).

When back biased the reverse leakage currents of Ge(Li) detectors are made negligible by cooling to liquid nitrogen temperatures so that the thermal generation of electrons and holes in the body of the counter and in the intrinsic region is kept to a minimum. The energy gap in the intrinsic germanium is approximately 0.7 eV, while visible light of wavelength 5900Å has an energy of approximately 2.1 eV. Thus a light tight container is essential to the correct operation of the diodes as detectors. To meet these requirements special chambers have been constructed using vacuum tight containers to prevent water and oil condensation on the cold detectors.

2.3 The Alloy Process

In fabricating such diodes the p-type germanium ingot is first alloyed with lithium as shown in Figure (4a) and then the intrinsic region is widened by drifting to produce the volume required as shown in Figure (4b). Figure (4c) shows the cross sectional view of this drifted diode. In the p-type material a gallium atom replaces one germanium atom in the lattice and because the gallium valence is three, a "hole" is left in the bond, thus giving the characteristic p-type quality. The concentration of the gallium atoms in the germanium determines the specific resistivity of the p-type germanium semi-conductor. The lithium atoms, on the other hand, form an interstitial dopant and combine with the gallium atoms to form an ionic bond. When the concentration of the lithium atoms is such that each gallium atom is compen-

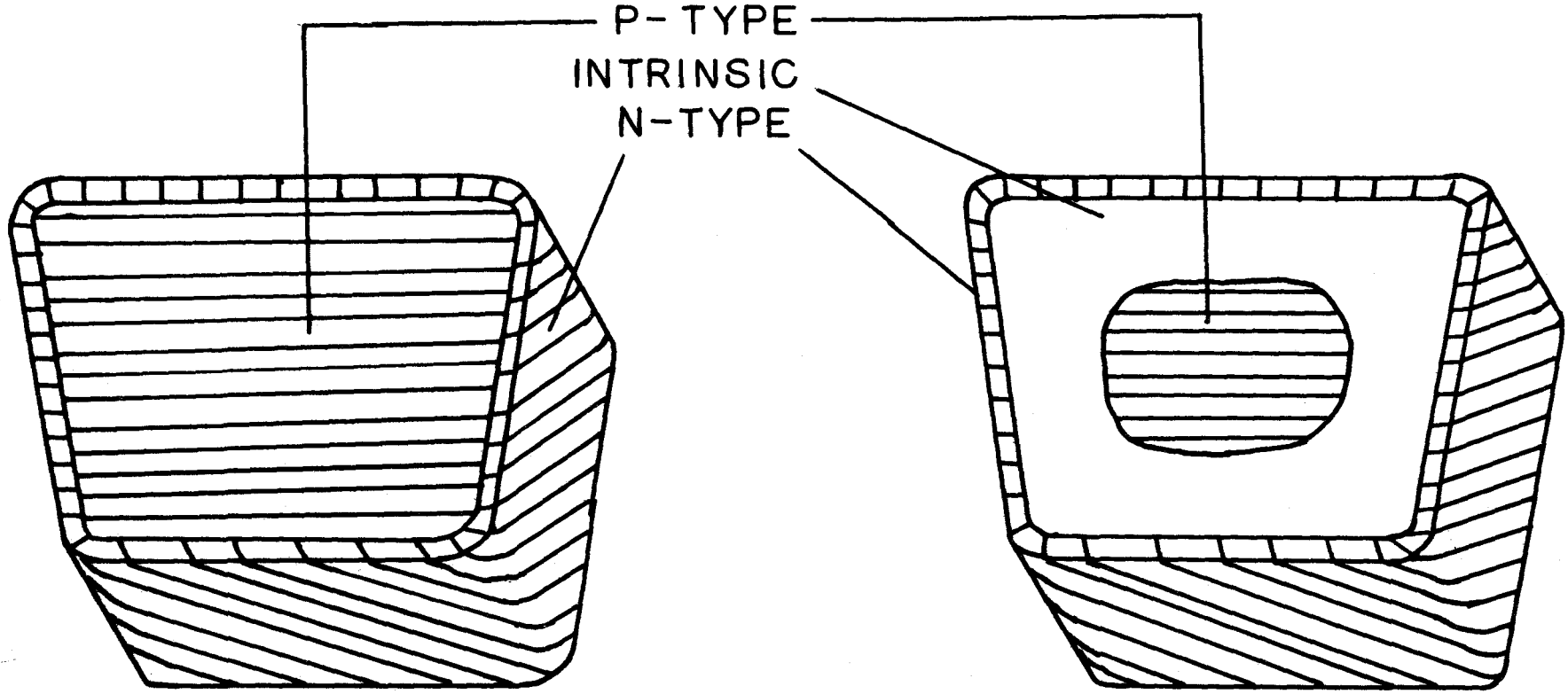

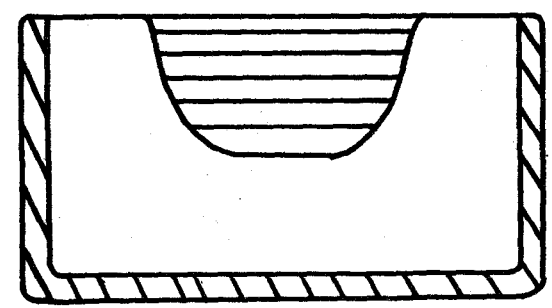

(c)

DIODE

FIG.4

sated or neutralized by a lithium atom then the material becomes intrinsic germanium with a specific resistivity of 60 Ω-cms at 25°C. If the concentration of lithium is increased beyond this compensating amount, the semiconductor becomes n-type with a sheet resistivity dependent upon the concentration. The alloying of lithium is usually done at 400°C, since the solubility of lithium in germanium at this temperature is sufficient to allow a high concentration of lithium to diffuse into the p-type ingot giving a sheet resistivity of ~0.01 Ω/□.

When the ingot has been alloyed and the resistivity is low, the diode is ready for drifting. However since the diode is at room temperature, the lithium atoms in the germanium form a super saturated solution, as described by Reiss et al [1], and as a consequence precipitation of the lithium will take place on defects in the crystal.

These nucleating centres for this precipitation are thought to be vacant germanium lattice sites occupied by lithium atoms[2]. As the lithium precipitates out of the solution the concentration goes down and the lithium is no longer active in compensating the gallium atoms, thus drifting slows down and if the resistivity goes above ~0.5 Ω/□ drifting virtually ceases.

2.4 The Drift Process

The technique for increasing the depletion or compensated region in which the lithium and gallium atoms form their characteristic ionic bond involves reverse biasing the diode and allowing about 200 watts of power to be dissipated in the diode. This reverse voltage and the elevated temperature (approximately 50°C) cause the lithium ions now to move through the material. The lithium ions are positively charged and the high mobility allows them to move towards the negative terminal. As the ions move they form ionic bonds with the gallium atoms thus increasing the compensated region.

To carry away the 200 watts generated, the diode is placed in a solvent, Freon TF. (B.P. 47.6°C). By vapour phase cooling this boiling liquid keeps the temperature of the diode fairly constant thus helping to regulate the power dissipated since the current generated in the diode is a function of the temperature. The actual temperature of the diode surfaces will be close to the boiling point of the Freon while internally the temperature will be higher[3]. The rate of drift is higher for the higher internal temperatures and this is evidenced when a completed diode is sectioned to show the internal drift region.

As the drift proceeds precipitation takes place and as a consequence the current-voltage characteristics deteriorate, i.e. current increases for a given voltage, and the drift rate decreases. This increased current is possibly generated in the precipitation nucleating centres. To keep the rate of drift as high as possible the number of precipitated lithium atoms must be kept to a minimum and the concentration of the lithium in the alloy layer must be as high as possible.

To achieve this situation after the precipitation has virtually stopped the drifting, the diode must be re-alloyed. This treatment will simultaneously re-dissolve the precipitated lithium and re-diffuse more lithium and will consequently bring the alloy concentration back to its original value since some lithium has been used to compensate the gallium in the depletion region. When a diode has been re-alloyed and has a practical size of approximately 4 mm of drift or intrinsic depth it can be prepared for the vacuum chamber.

2.5 The Packaging Process

In the high-power drift the currents are normally quite high $\sim$ 1.0A. This current constitutes a space charge in the depletion region and thus the drifted lithium atoms will compensate these charge carriers, with the disadvantage that when the current is decreased there is an excess of lithium in the intrinsic region over and above the true compensating concentration. These n-type centres must be removed to give the depletion region as high a resistance as possible i.e. low leakage current. In order to take as many of these lithium atoms out of the depletion region as possible a low-power drift is necessary. The power involved in this "clean up" drift is of the order of a few watts, and the time of drift is determined by the diode characteristics and is an an experimental problem rather than a theoretical one.

When the "clean-up" drift has been finished the exposed surface must be thoroughly cleaned but here the real problem is only on an experimental basis at the present time. The treatments involved have been many but the best one found to date both in this laboratory and elsewhere[4] will be discussed later.

CHAPTER III

DETECTOR FABRICATION

3.1 Preparation of Germanium

The basic material used in preparing the gamma ray detectors was float-zoned, size No. 4, p-type germanium ingot, grown in the ⟨111⟩ orientation. These ingots had a resistivity of $\sim 40\,\Omega$-cms; minority carrier life time of $\sim 300\,\mu$sec; maximum and minimum dislocation density 2600 pits/cm^3 and 2300 pits/cm^3 respectively and were obtained from Sylvania Electric*. The cross-sectional area of each 300 gm ingot used was ~ 8.5 cm^2. "No-Load" cement is used to hold the germanium on a graphite plate in order that it may be cut to the desired length by a diamond wheel saw. The cutting speed can vary but 1 mm/min. is average and if care is taken this part of the process causes little crystal damage.

When the ingot has been cut, the piece desired is removed after re-heating the graphite plate and melting the compound. In order to prepare this piece for the next part of the procedure, a lapping tray was made, complete with running water to remove residue while lapping. The lapping papers are grits No. 240, No. 320, No. 400 and No. 600 obtained from Fischer Scientific Co. All sides of the piece are then lapped in

---

* Sylvania Electric Inc., Chem. and Met. Div., Towanda, Penn., U.S.A.

the 240 grit paper to remove all cutting damage and the remaining cement. The easiest technique is to lap each side in one direction and then when lapping on a new paper of finer grit the side should be turned through 90° so that all new scratches are perpendicular to the previous ones. This makes it easy to see how the lapping is progressing. When the final 600 grit paper is used the surfaces still have a matte finish but as this paper is used repeatedly these scratches become finer. At this point in the process all six sides of the ingot have been lapped on the 600 grit paper and then it is cleaned in a methanol, trichloroethylene, methanol series of washes to remove grease and water. The reagents used are all electronic grade products from Fischer Scientific Co. and are kept in standard wash bottles. Now the piece of germanium is ready to be alloyed.

3.2 Alloy Technique

In the theory section of Chapter II it was pointed out that the required temperature for diffusing lithium into the germanium to obtain the optimum characteristics in the n-type alloy region, was $\sim 400^{\circ}C$. The technique[5] employed and originated in this laboratory allows the lithium to be simultaneously electroplated onto the germanium and diffused into it at the desired temperature.

The apparatus as shown in Figure (5) includes a muffle furnace, a graphite crucible and a rigid clamp to hold the ingot to be alloyed. The mixture of 50% by volume lithium chloride and 50% potassium chloride is placed in the crucible and the temperature is raised enough to just melt this mixture. This temperature is $\sim 400^{\circ}C$ but the main criterion for setting the furnace temperature is that the mixture is just a few

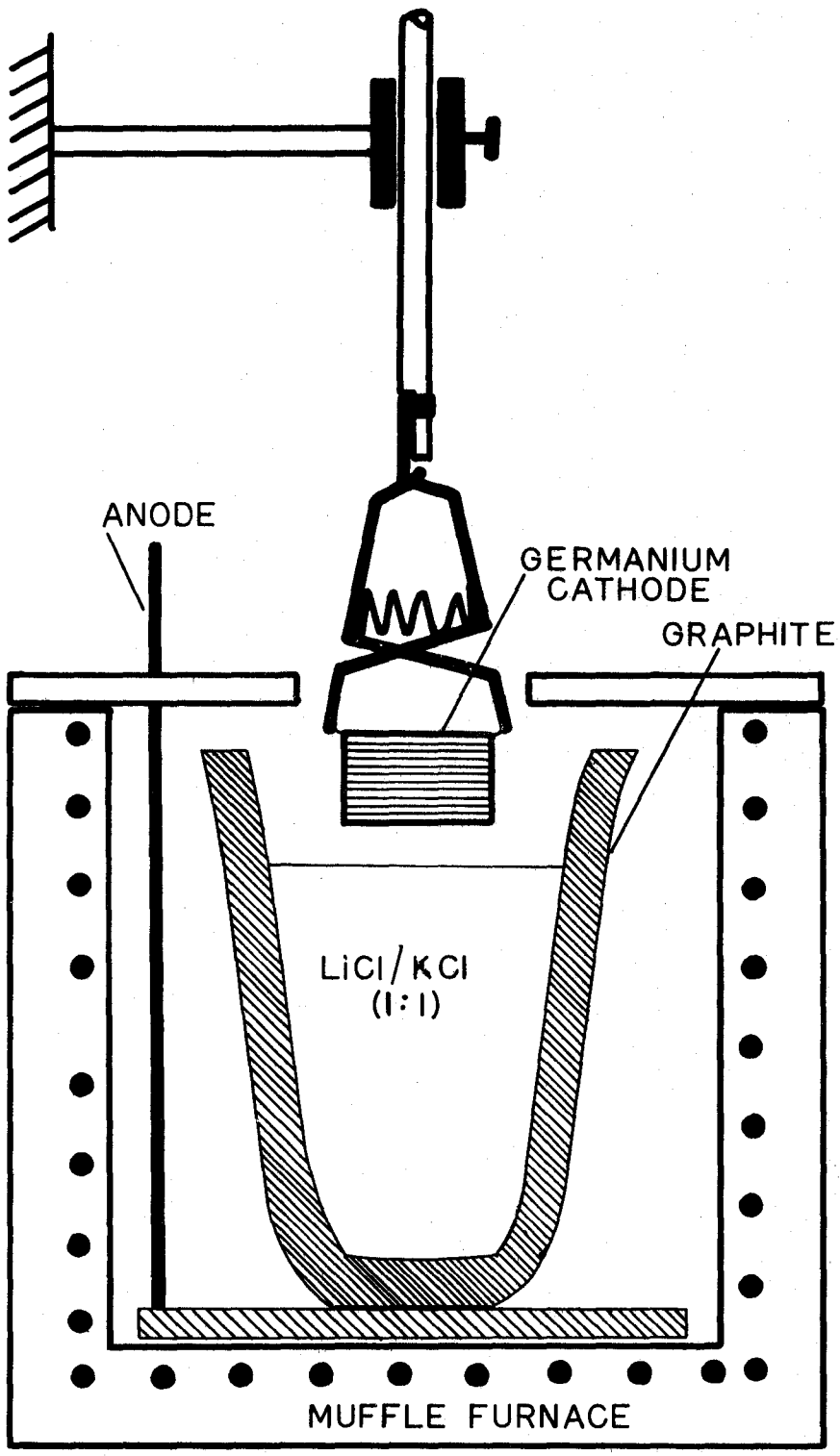

ALLOYING BATH

FIG.5

degrees above its melting point. This condition has proven very important in producing good detectors.

When the temperature is stabilized a scum of graphite and dust may form on the surface of the melt. This can be removed with swabs of glass wool.

The clamp which holds the germanium is a standard battery clamp* and the contaminants and plate material are burned off with an oxy-gas flame. At this stage, when the melt and the germanium are prepared, care must be exercised in warming up the ingot since it is very susceptible to damage by thermal or mechanical shock. The clamp and ingot are positioned about one foot above the open furnace and maintained there for five minutes. Then the clamp is lowered to six inches for five minutes, then to 3 inches for another five minutes and continuing until the ingot is a few millimeters above the surface of the melt. It may be left here for ten or fifteen minutes to ensure the temperature has been stabilized again. The alloying power supply is shown in Figure (6) and is capable of delivering up to 6A at 100V or 2A at 500V. In the alloying procedure the ingot is the cathode while the graphite crucible is the anode thus the positive lithium ions will be attracted to the germanium according to the standard electroplating technique. The ingot is lowered into the lithium melt until its top surface is $\sim$2 millimeters above the surface of the liquid salt solution. The voltage is turned on ($\sim$6V) and depending upon the size of the ingot a specific current is maintained for a given time. As an example of the current and time required to give a suitable alloy, consider a piece of germanium 2 cm high by 8.5 cm^2 in cross-section area. This piece will be alloyed at 3 amps for 5 minutes at the lowest temperature possible i.e. 400°C. These conditions will produce an alloyed depth of $\sim$0.7 mm with a sheet resistivity of

* Obtained from the Canadian Tire Corporation

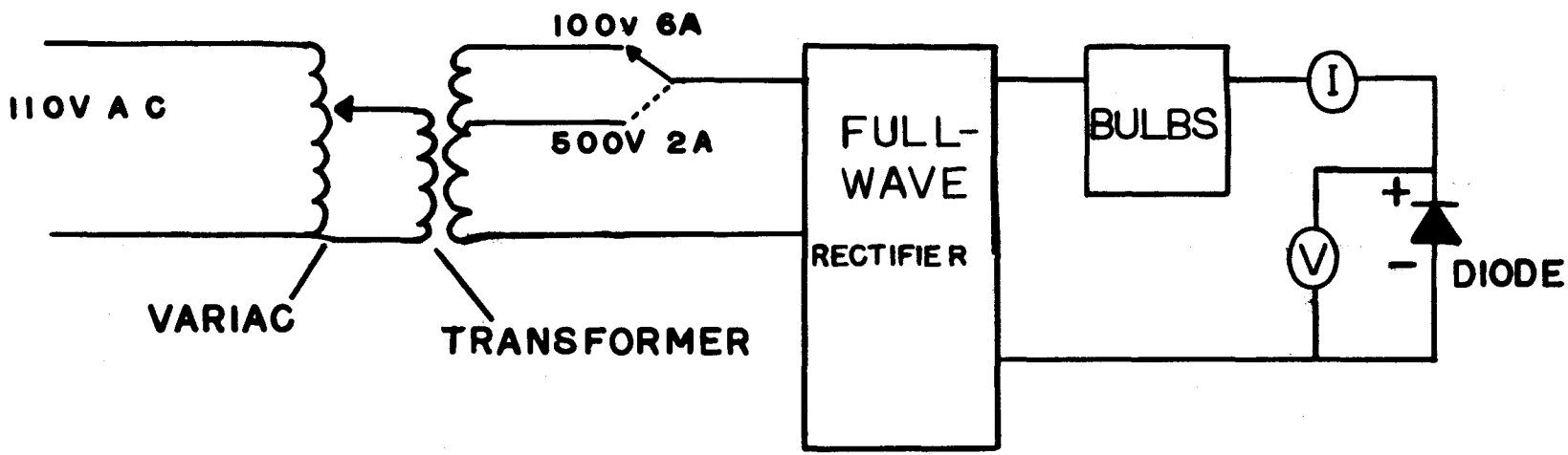

DRIFT CIRCUIT

FIG. 6

$\sim 0.03\,\Omega/\square$ when measured with a 4 point probe[6]. The current density is therefore usually $\sim$100 ma/cm^2 when the area refers to the total area of the five sides of the ingot immersed in the solution.

The low temperature and the short time used give a very thin alloy as opposed to a temperature of 450°C with a current of 3 amps and a time of thirty minutes which will give an alloy depth of 2-3 mm for a device of the same total area. All detectors which have been alloyed under these low temperature conditions have worked well, while those with thick alloys due to the higher temperatures have not had as good a success rate.Some of these results are shown in Table I. Table IA refers to those detectors with thick alloys which were given a final surface cleaning of doubly distilled water. Table 1B refers to the "thin alloy" detectors cleaned with a final rinse in methanol. In fact the success rate of the low temperature alloy is six useful detectors for six starting ingots.

To remove the hot diode now from the alloy bath involves wrapping it directly in glass wool. Care must be taken to avoid long contact with air at room temperature and for this purpose the glass wool is used. For example in about 50 alloy procedures only twice were the diodes cracked due to thermal shock. When the diode is in the wool the molten salt on its surface must be quickly removed by rubbing with the glass wool to avoid cracking as the salt solidifies. The diode is given about thirty minutes to cool down to room temperature and then the remaining salt is lapped off the device. The uppermost side of the germanium is not electroplated with lithium since it is held out of the melt. However in most of the allowing procedures some molten salt does flow over

TABLE I

Detectors Fabricated

		A (Distilled Water)					B (Methanol)				
	1	2	3	4	5	6	8	9	10	11	12
Height (cms)	2	1.25	5	5	2	1	2	1	2.5	1	1
Temp(^{o}C)	410	-	-	480	440	Low	410	410	410	420	400
Current (amps)	1.5	0.33	-	2.5	1	2	2	1.75	3	1.75	1.1
Time for Alloy (min)	30	35	-	20	15	5	15	4	10	6	5
Depth of Alloy (mm)	1	-	1.5	1.9	1.5	1.5	1	0.75	<1	1	<1
Resistivity $\Omega/\square$	good	good	0.04	0.01	0.03	0.02	0.05	0.04	0.03	0.08	0.08
Final Drift Depth (mm)	8	7	10	4	6.5	6.5	4	5	4	4	3
Final Alloy Depth (mm)	2	4	3	5	2	2	1	1	2	1.5	1
Resolution at 1 MeV (keV) (FWHM)	8	9	20	17	-	-	8	8	8	8	10

the edges of the ingot onto the top surface and as a consequence alloys into the ingot. This top surface must be lapped down to get this surface alloy off.

To check the actual depth of alloy obtained, the diode is placed in a beaker containing a $CuSO_4$ solution and a six volt back bias is applied across the diode i.e. negative terminal on the p-type germanium region and positive terminal on the lithium alloy (n-type) region: This plating technique delineates the alloyed and p-type regions extremely well. When the lapping and copper plating of the junction region surface is complete, the other five sides are lapped clean and the sheet resistivity is measured on a four point probe[6]. Usual resistivity measurements are shown in Table I.

As long as the alloy resistivity is less than 0.2Ω/□ the diode is put in the drifting apparatus which forms the next step in the total fabrication process.

3.3 Drift Process

An important step just before drifting involves cleaning the junction surface to prevent surface leakage. The diode is washed in the methanol, trichloroethylene, methanol rinse cycle and then the junction surface alone is etched in an acid solution of 3 parts concentrated nitric acid, 1 part red fuming nitric acid and 1½ parts hydrofluoric acid. The whole diode can be etched but it becomes slippery and hard to handle consequently only the one face is etched. When the diode has been held in the etch for about 30 seconds it becomes quite hot, at this time it may be quenched with methanol and the surface can be checked visually for scratches and pits. It is usually necessary to repeat this etching

cycle 3 or 4 times before the surface is satisfactory. To avoid oxidation, air must be kept from the surface until the acid has been thoroughly quenched with methanol. Now the etched diode is ready to be put in the drifting apparatus. This apparatus is shown in Figure (7) and as discussed above in the theory section the cooling liquid used most frequently in this laboratory, is Freon TF. At present Pentane is being tested to see if the lower temperature of its boiling point causes a marked decrease in precipitation rate. It appears that there is a noticable effect; however only one counter has been produced using this liquid and no conclusions can be drawn.

The power supply for the drifting of the lithium is the same one as used in the alloying process. However now, series light bulbs are used to control the voltage on the diode. Essentially the bulbs act as an automatic variable resistance which increases as the diode draws more current through the circuit. Thus, as the diode resistance decreases, due to precipitation, the bulbs have a compensating effect which keeps the current below break down levels.

When the apparatus is in position and the power is connected so as to back bias the diode, the initial voltage is raised very slowly with the maximum resistance in the control unit. The voltage is raised until the Freon starts to boil around the diode; then the power is stabilized for a few hours to allow the thin depletion region to drift under the influence of the small field. In the Freon (B.P. 47.6^{o}C) and with the characteristic alloys in Table IB, this power level in the diode will be approximately 50 watts where the voltage is 100V with $\sim$ 500 ma of current being drawn.

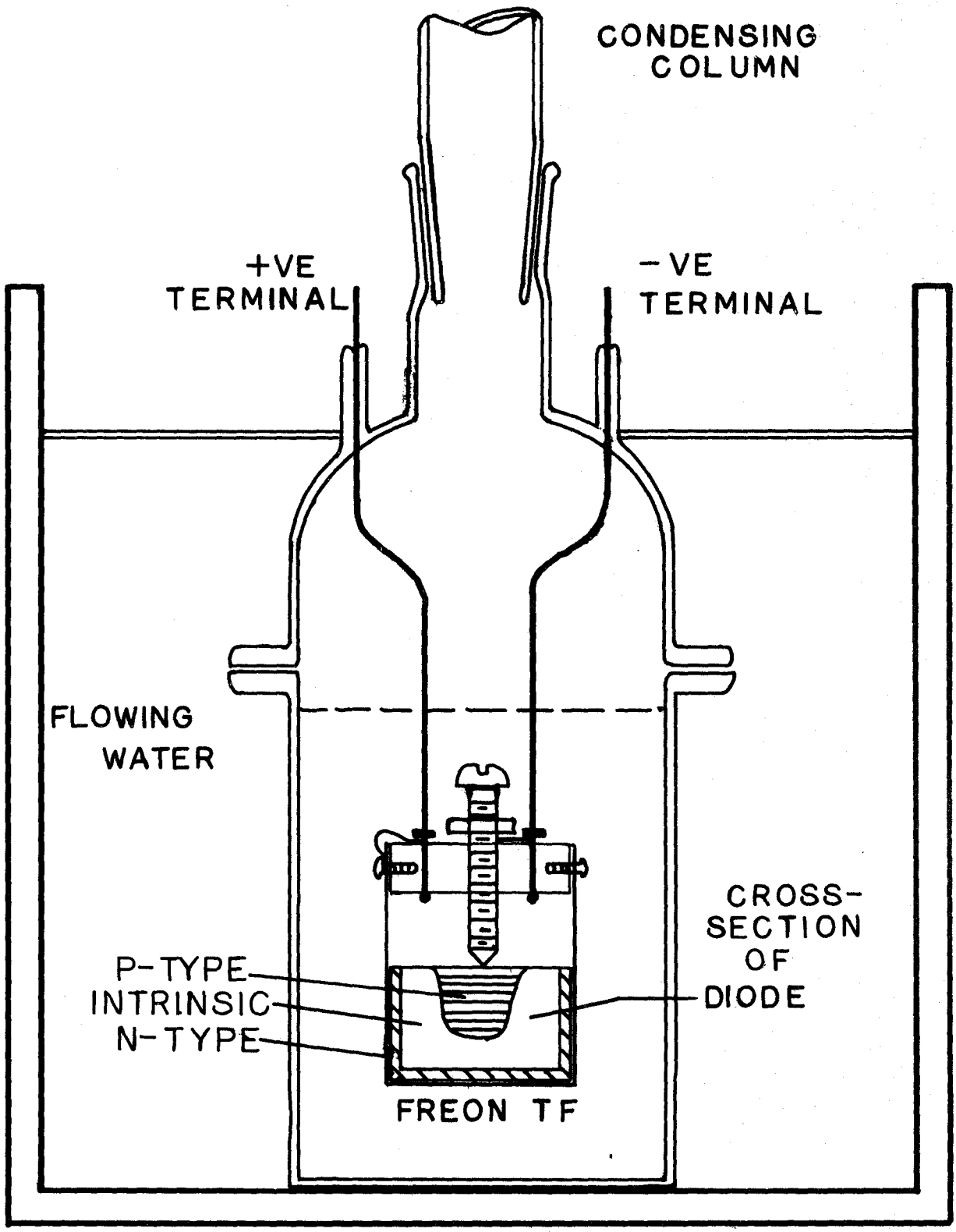

DRIFT APPARATUS

FIG.7

After a few hours the power is increased to 200 watts or greater with characteristic voltage and current of 250V and 0.8 amps respectively. The best way of finding the optimum power for drifting is to increase the power slowly while adjusting the light bulbs as the current rises, so that when break down occurs the resistance in the bulbs will be sufficient to drop the voltage on the diode and thus little or no damage is done. After checking the diode in the above manner the power is dropped below the maintaining voltage, for breakdown, in the diode and then raised to within approximately 30V of the original break down voltage. The diode can now be left for a few days without any attention at all.

As stated above, normal resistivity measurements of the alloy region performed immediately after alloying, show the sheet resistivity to be approximately 0.03$\Omega/\square$ but the value slowly rises with time while drifting. As this occurs the back biasing characteristics of the diode deteriorate i.e. for a given voltage the current increases and when the value of resistivity reaches approximately 0.5$\Omega/\square$ drifting almost ceases. This increase in resistivity is evidence that the lithium is precipitating in the inhomogenities in the material and is thus not available for the compensation of the gallium ions.

A diode is left drifting for approximately one week and at the end of this period the voltage has usually dropped to 150V with 2 amps being drawn from the power supply. The voltage decrease on the diode is due to the increase in voltage across the light bulbs. The diode is now taken out of the drift apparatus and the depth of drift is checked by the copper plating technique and the resistivity is checked

with the four-point probe[6]. At this time the resistivity has usually risen to between 0.1 and 0.2 Ω/□ and the drift depth or depletion region is approximately 4 mm.

To give this device optimum characteristics for use as a gamma ray detector, it has been found that the resistivity should be as low as possible; thus the device must be alloyed again under similar conditions for half the time that was used in the initial alloy procedure. This keeps the alloy depth small while lowering the sheet resistivity of the alloy surface. The diode is placed in the drift bath again for a few hours at high power but the voltage-current characteristics are usually not as good as the initial ones, partially due to the fact that the intrinsic region is larger now and this allows more thermally-generated hole-electron pairs to contribute to the current for a given voltage. After this few hours of drift the device is ready for a "clean up" drift and can then be packaged in a detector chamber.

3.4 Packaging Process

This part of the process is the one which causes most trouble at present, but consistent results are now available which prove that the technique is adequate for obtaining detectors which can give 12 keV (FWHM) resolution for 6 MeV gamma rays.

A clean up drift is essential for the proper performance of a detector. This has been treated in the theory section and only the actual mechanics are given here. To clean up the device the voltage on the diode is dropped in steps of approximately 25 volts from the high-power level discussed above. At each step the characteristics take about thirty minutes to stabilize. The final voltage should be approximately 50 volts and should be stabilized for about an hour. The temp-

erature of the device at this time will be approximately 12°C since the Freon is being cooled by the cold running water as shown in Figure (7). Thus it takes between three and four hours to complete this procedure. Many other experimenters[7] use much lower temperatures with higher reverse voltages and smaller currents. One example is given of a reverse bias of 1000V drawing 5 ma for about 5 hours[8].

When the "clean-up" drift is completed the device is removed from the drifting bath and very thoroughly lapped on all surfaces while on the junction face the finest paper, grit No. 600, is used until a very good surface is achieved - experience is the only teacher here. The methanol, trichloroethylene, methanol rinse cycle is used again but very thoroughly now until all contaminants are removed. The etch is renewed and this time three baths of methanol are prepared for the final rinse after etch. Before the device is etched the chamber is prepared and the dry He gas and an indium-gallium eutectic mixture are close at hand. The eutectic mixture is approximately 50% indium by volume and 50% gallium and it allows a good ohmic contact to be made to the p-type germanium of the detector. Now comes the critical few minutes of the 2 to 3 week process. The detector is held, junction face down, in the etch and the usual technique is followed using the first methanol bath. When the experimenter is satisfied that a good surface has been obtained he then rinses the whole device in the remaining methanol baths in succession but air (water vapour) must not come in contact with the surface between dips. While holding the detector in the final methanol rinse the bath is placed beside the chamber holder and when everything is ready, a jet of helium is used to remove the methanol from the surface. How-

ever many attempts must be made with this latter procedure before a satisfactory surface is achieved.

The indium-gallium eutectic mixture is placed on the clean surface where the contact is to be made to the p-type core. Helium gas is blown on the junction surface throughout this whole procedure. The detector is placed in the chamber holder and the cap is bolted into place as quickly as possible to prevent contamination of the surface. The chamber is then quickly evacuated with a mechanical oil vacuum pump. A molecular sieve pump is then applied to the chamber with the mechanical pump out of the system to avoid contamination by oil. On some chambers another pump can be activated when the sieve has achieved its ultimate vacuum. This pump is an ion pump which evacuates the chamber by ionizing the air molecules and adsorbing them on a titanium sponge.

It has been found in the test apparatus that the sieve alone can hold an adequate vacuum in the test chamber for a period of 12 hours at which time it is only necessary to add more liquid nitrogen to the dewar around the molecular sieve container. The sieve material is type 5A, molecular sieve obtained from Linde.

3.5 Detector Chamber

A diagram of a Test Chamber is shown in Figure (8) with the detector shown as a cross-section, in the holder. As soon as the aluminum cap has been bolted into position a small reverse voltage of approximately 10 volts, is applied to the detector as a low power clean up drift. When the best possible vacuum has been achieved in the vacuum chamber liquid nitrogen is added to the stainless steel cold finger to cool the device. The detector is now in a light tight,evacuated chamber

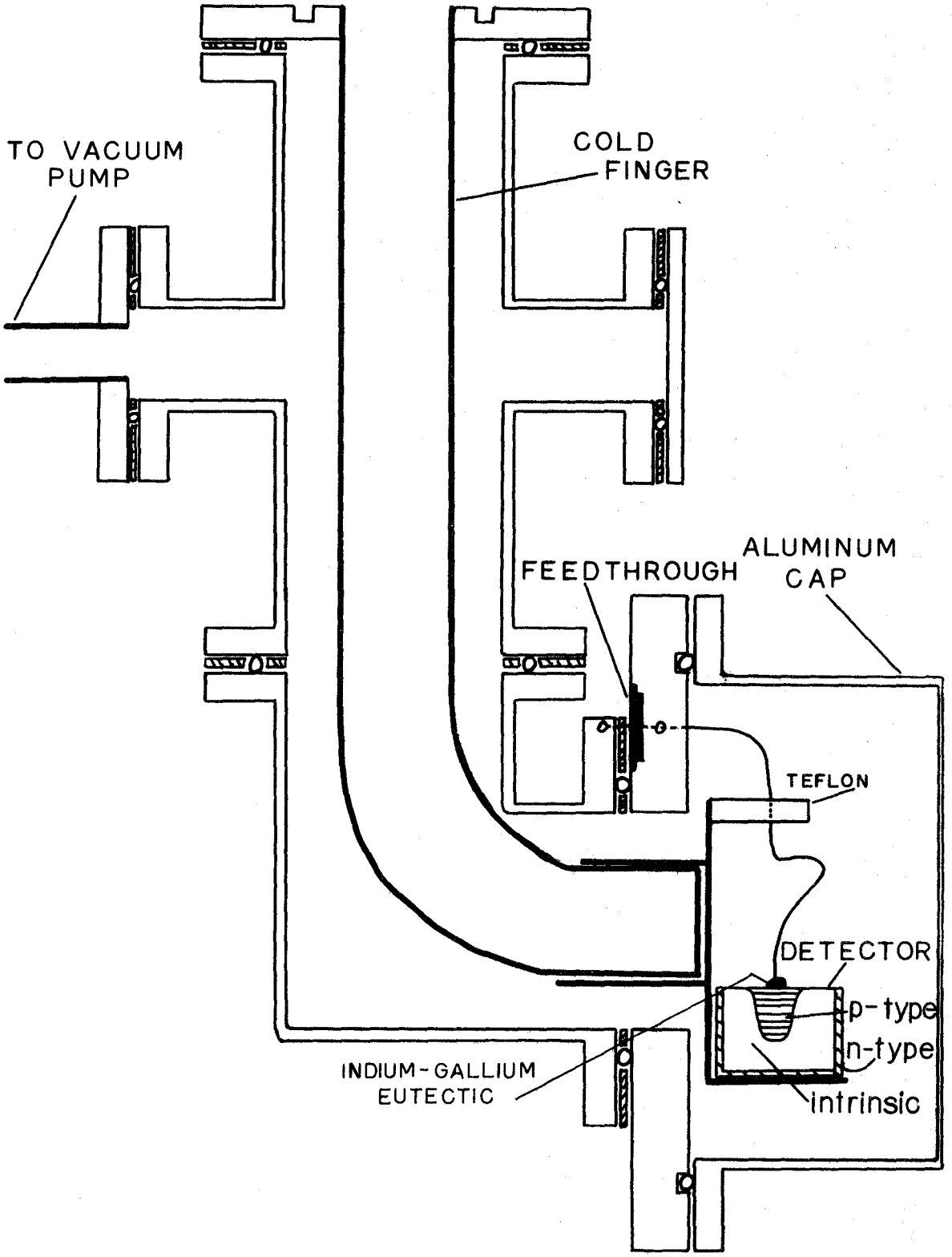

DETECTOR TEST CHAMBER

FIG. 8

and is at a temperature very close to 77^{O}K. and provided that the junction surface has been treated properly the detector is now ready for leakage current tests and subsequent operation.

CHAPTER IV

DETECTOR CHARACTERISTICS

4.1 Response to Gamma Rays

The response of a lithium drifted germanium detector to gamma rays is quite complicated in comparison to that for charged particles. The charged particle loses energy in direct collisions with the electrons of the semi-conductor or gas while the gamma rays lose energy by: 1) the photoelectric effect which causes an electron to be emitted from an atom after the total absorption of the incident gamma ray; 2) the Compton effect in which a gamma ray is scattered by an electron and in so doing loses energy to this electron; 3) the pair production effect which annihilates a gamma ray in the field of a nucleus and creates an electron-positron pair with total kinetic energy E given by

$$E = E_{\gamma} - 1.022 \text{ (MeV)}$$

The total absorption coefficient for gamma rays in germanium is shown in Figure (9).

When the total energy of a gamma ray has been absorbed in one or all of the above processes the energetic electrons and holes lose their energy in subsequent collisions creating many more electron-hole pairs. It takes approximately 3 eV of energy to create a pair. These new charge carriers now form the energy proportional pulse which is amplified and analyzed. However, to further complicate the analysis of gamma rays, the crystal lattice of the detector itself can inhibit the collection of these charge carriers.

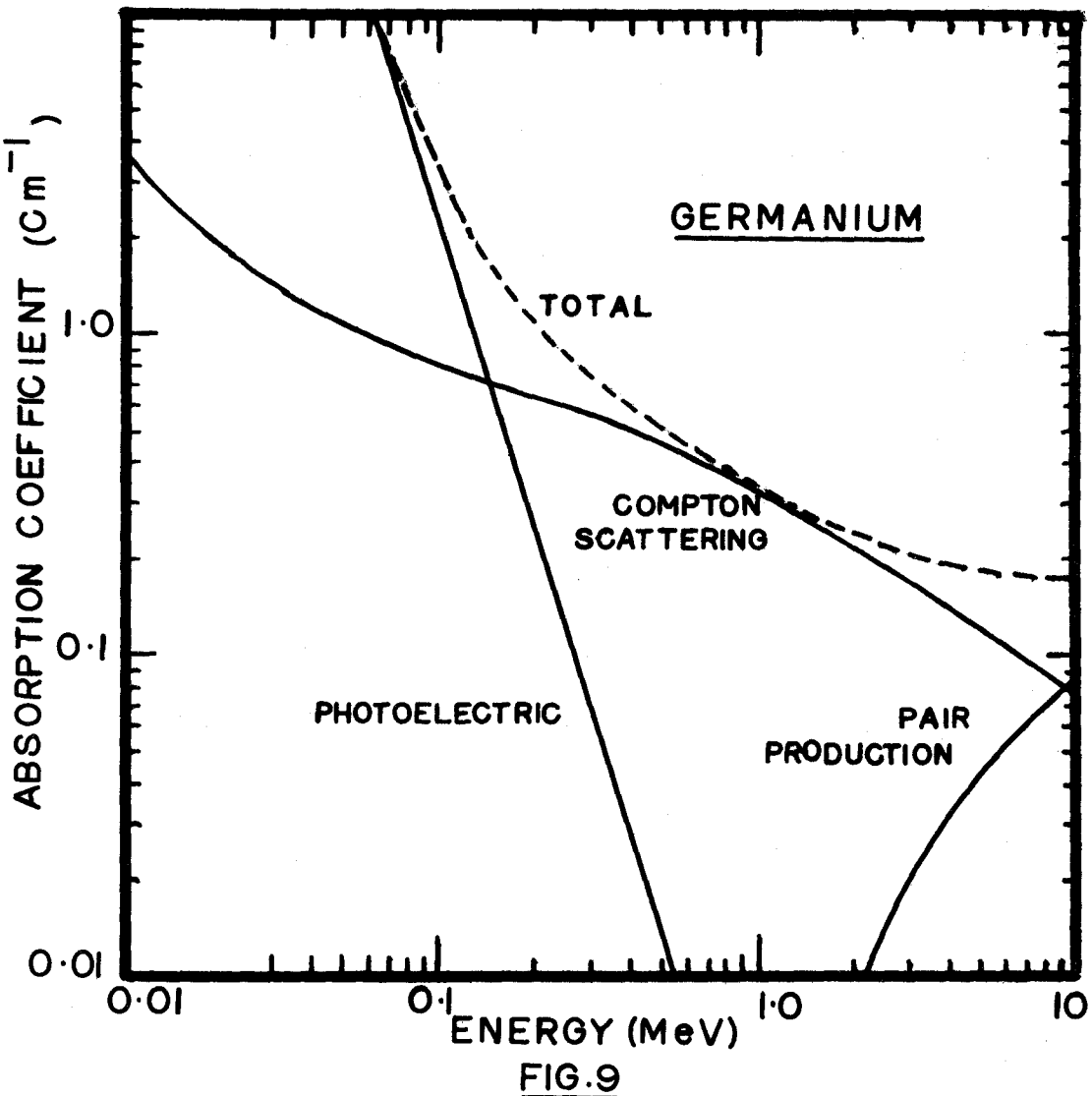
GERMANIUM
TOTAL
COMPTON SCATTERING
PHOTOELECTRIC
PAIR PRODUCTION
ABSORPTION COEFFICIENT (Cm⁻¹)
1·0
0·1
0·01
0·01
0·1
1·0
10
ENERGY (MeV)

FIG.9

The intrinsic semi-conductor volume, obtained by the drifting technique described, is the sensitive volume of the detector and it is in this region that the high electric field exists. If the semiconductor is very pure intrinsic material then at low temperatures the only currents generated will be due to thermal agitation. However the intrinsic material produced in fabricating detectors is not a pure lattice structure but has many impurity centres either on original lattice sites, or on interstitial sites. These impurity centres can become ionized either by the donation of an electron to the conduction band or by accepting one from the valence band and thus introduce localized energy levels usually in the forbidden gap. These impurities refer both to the dopants used in fabricating the device, i.e. (gallium on germanium lattice sites and lithium on interstitial sites) as well as to other inhomogenities such as a lithium atom on a germanium site. These latter localized centres tend to reduce the current formed when a gamma ray ionizes the material. They act as traps at which holes or electrons become localized subsequently returning to the valence or conduction bands respectively, in a relatively short time or they may act as sites at which electrons and holes annihilate and are thus removed from the current pulse entirely. Thus, between the time the pulse is formed and amplified there can be much distortion of the true energy spectrum depending on the impurity levels in various parts of the device. Consequently appropriate adjustments have to be made to the integrating and differentiating time constants of the amplifying system[9]. In this analysis each detector is completely different because of different intrinsic volumes, different heat treatments, and different

starting ingots, all of which introduce varying impurity levels. However in this work the last six detectors have been fabricated from different starting ingots and all have been of different sizes, and each of these has had a resolution of between 8 and 9 keV when measuring the 1114 keV transition of Zn^{65}. So it seems that the impurity levels have been kept to an adequate level both by obtaining good ingots and keeping the heat treatments to a minimum.

4.2 Characteristics

When a good detector has been packaged certain measurements can be made on it to test its quality. These measurements are:

1) leakage current versus voltage,

2) resolution versus voltage .

To check the leakage current under reverse voltage conditions a simple test circuit was built which incorporated a grounded current meter in series with a floating voltage and the grounded detector. The leakage current through the circuit itself was 1×10^{-9} amps. Figures (10) and (11) show leakage current, resolution and the ratio of photo-peak to Compton distribution, versus voltage for two different detectors. These curves are characteristic of the detectors fabricated in this laboratory. If the negative sloping part of the resolution curves is considered it will be seen that the photo-peak ratio is increasing in the same voltage range. This is due to the increasing charge collection efficiency as the internal field rises. When the voltage for the minimum in the resolution curve is reached it can be inferred that the photo-peak ratio will be a maximum from statistical considerations since the source strength was constant throughout the measurements. As the voltage is increased

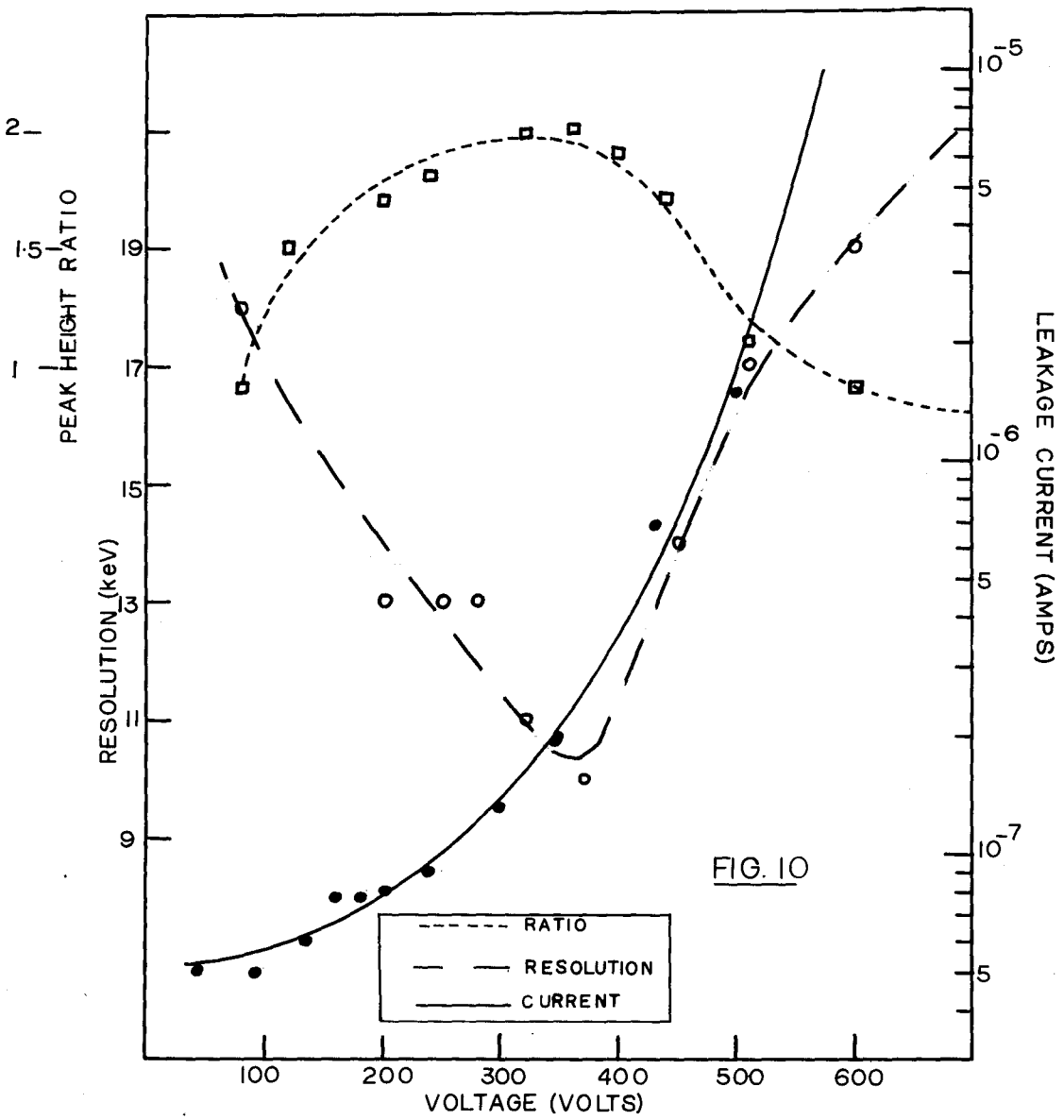
PEAK HEIGHT RATIO
2
1·5
1
RESOLUTION (keV)
19
17
15
13
11
9
LEAKAGE CURRENT (AMPS)
10^{-5}
5
10^{-6}
5
10^{-7}
5
100
200
300
400
500
600
VOLTAGE (VOLTS)
RATIO
RESOLUTION
CURRENT

FIG. 10

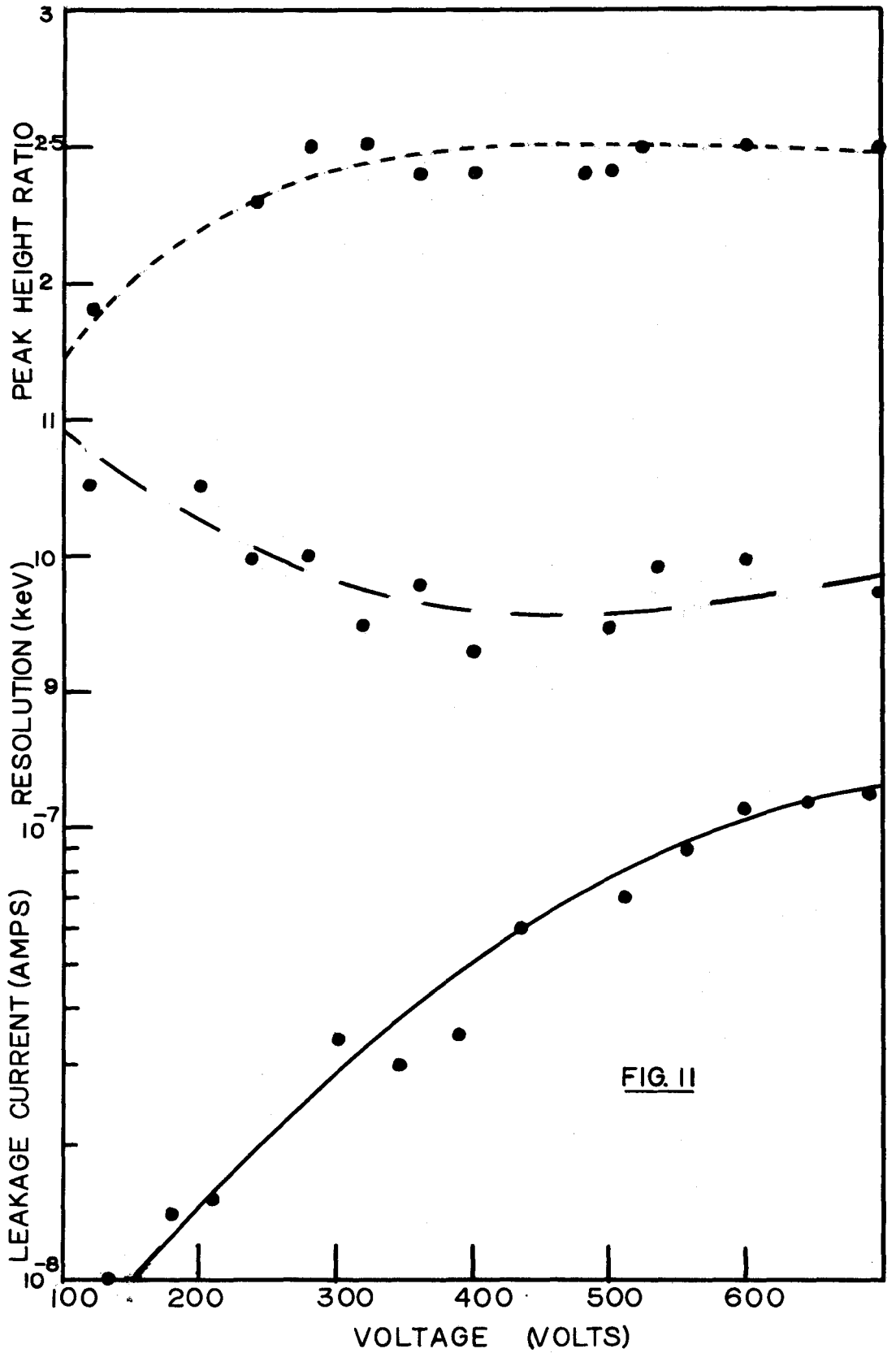
PEAK HEIGHT RATIO
RESOLUTION (keV)
LEAKAGE CURRENT (AMPS)
3
2.5
2
1
10
9
10^{-7}
10^{-8}
100
200
300
400
500
600
VOLTAGE (VOLTS)

FIG. 11

above the "peaks" in Figure (10) it will be seen that the characteristics begin to deteriorate. This change in resolution is mainly due to the increased noise level caused by the excessive leakage current ($> 2.5 \times 10^{-7}$ amps). This current can be attributed probably to both surface contaminants and internal generating sites but as stated elsewhere only the surface currents can be minimized after fabrication. In Figure (11) it can be seen that the leakage current does not rise as sharply as that in Figure (10) and as a consequence the resolution curve is seen to remain low over a very wide range of voltages.

The contribution to the leakage current which can be minimized after fabrication is that part due to junction surface contamination. The investigation carried out by Armantrout[4] shows that the energy states at the junction surface are very dependent upon treatment techniques. On a good surface the field across the depletion surface must be constant showing that it is indeed an intrinsic material. His measurements show how the n-typeness or p-typeness of this surface changes with time. If the surface reverts to a p-type material then there will be available charge carriers in the form of holes, in the depletion region which will lead to an increase in the leakage current. He goes on to show that the methanol baths used in the surface treatments lead to the best surfaces and lowest values of leakage currents.

While the actual measurements of the field across the intrinsic surface carried out in the above investigation, were not made in this work, different surface treatments have been used. At the beginning of the investigation a surface treatment was used which included the same concentration of etch as used in all the treatments and a rinse in

double distilled water which was blown off the surface with dry helium gas. The gas was not kept flowing over the device. One spectrum of Zn^{65} obtained with a detector fabricated in this way is shown in Figure (13). This detector had as good resolution and efficiency as the newer detectors packaged using the methanol rinses. Thus there may have been quite a bit of lucky timing involved with the distilled water rinse since no systematic results were achieved. However it cannot be said that the "methanol" surface treatments alone helped produce more consistent results because the alloying techniques were changed also. A test has been performed on the "new" detectors in which distilled water was used as a final rinse. These leakage currents were an order of magnitude greater at a given voltage than those from the methanol rinses.

By copper plating one of the first detectors fabricated in this laboratory, it was found that the depleted or intrinsic volume was approximately 90% of the total volume of the ingot. To insure that this depleted volume was indeed "active" a specific counting experiment was performed. This experiment involved firstly obtaining the strength of a specific source with a NaI(Tℓ) scintillation counter using data taken from Heath's[10] experiments. The NaI(Tℓ) data obtained in counting the source was corrected for efficiency and solid angle and the source strength was calculated accordingly. Secondly the same source was counted with the Ge(Li) detector and its active volume calculated. This volume obtained by the counting experiment agreed well with the volume calculated from the copper plating technique.

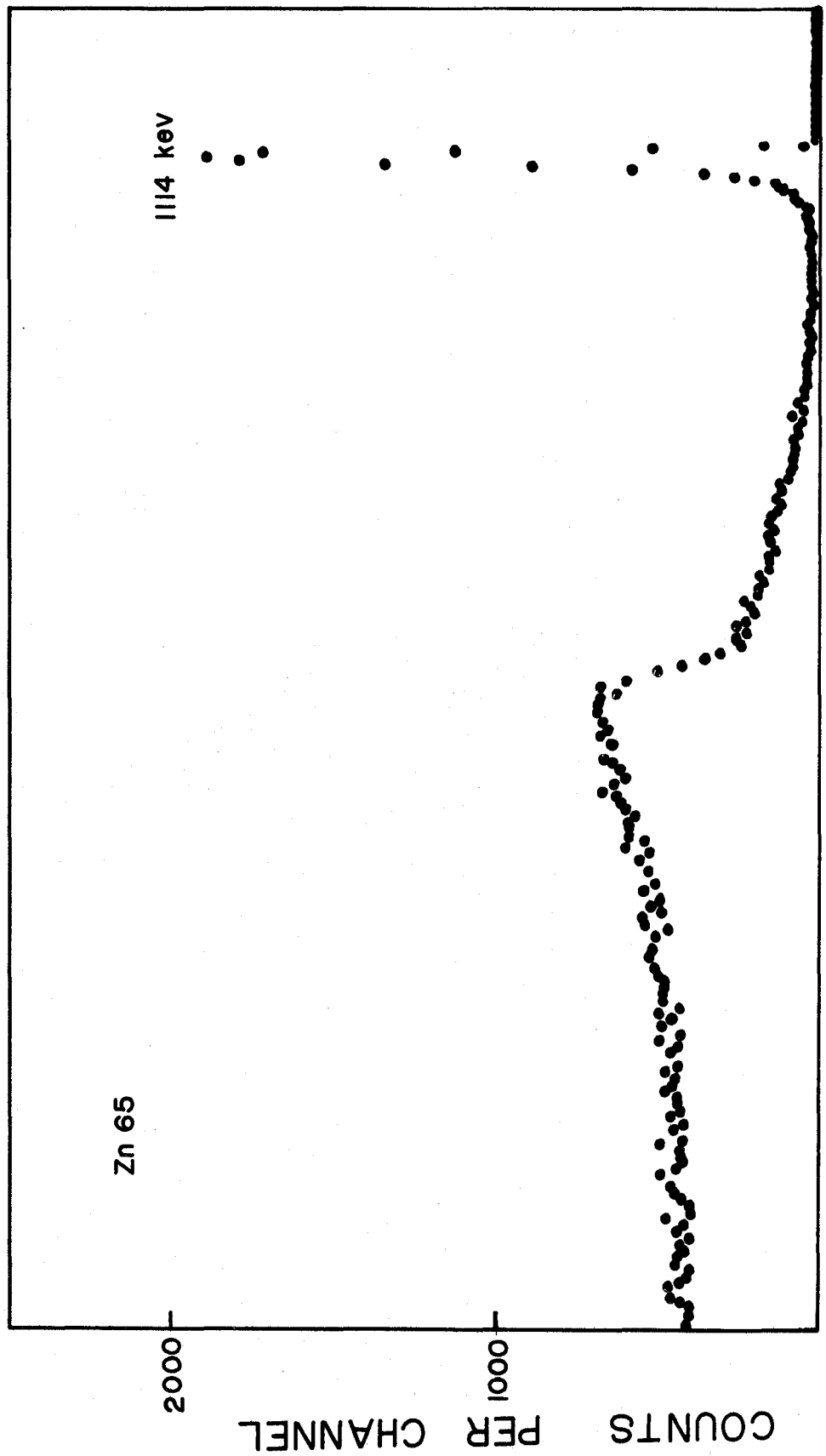
1114 kev
Zn 65
2000
1000
COUNTS PER CHANNEL
500
600
700
800
CHANNEL NUMBER

FIG.13

The principal reasons for producing large volume counters are to improve the solid angle and interaction probability, to insure that most electron ranges are considerably less than the dimensions of the active volume, and to enhance multiple events. The latter two, result in an improvement in photo fraction i.e. the ratio of the number of events in the full energy peak to the total number of events detected. A portion of the spectrum of the 1114-keV Zn^{65} transition is shown in Figure (13). For this energy the height of the photo-peak is about 5 times that of the Compton distribution and the peak contains approximately 3% of the total number of all interactions in the counter. This dramatic increase in the photo-efficiency over small volume counters[3] where the peak height is of the order of the Compton distribution, clearly demonstrates the value of large volume detectors. To find the contribution of multiple events and increased electron stopping efficiency, a series of measurements to determine the photo fraction and photo-efficiency were made. The relative photo efficiency for a 10 c.c. detector is shown in Figure (14). To obtain this relationship sources were used for which the decay scheme was known. Only for the low energy region was it necessary to employ mixed sources and NaI(Tℓ) measurements in order to tie the various points to a common scale. For comparison with the observed data, curves of efficiency versus E^{-1}, E^{-2} and E^{-3} are also shown. Theoretical calculations[11] of the photo electric cross sections suggest that the efficiency should follow approximately $E^{-2.5}$ in the range from 0.1 to 0.5 MeV and approximately $E^{-1.5}$ in the range from 0.5 to 3 MeV. It will be noted that the efficiency does not drop off as rapidly as predicted indicating that multiple events are contributing to the photo-peak area. A similar measurement conduct-

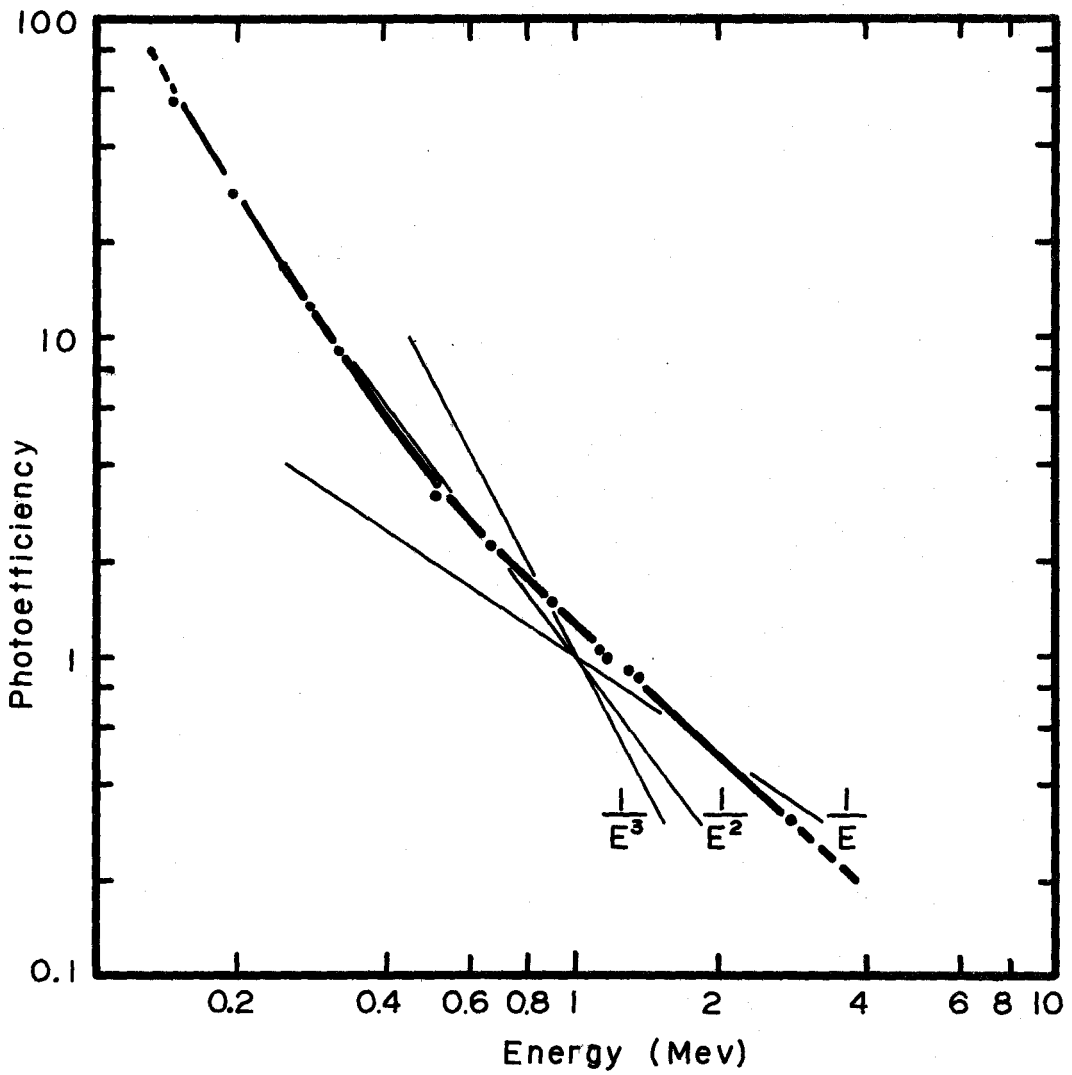
100
10
1
0.1
Photoefficiency
0.2
0.4
0.6
0.8
1
2
4
6
8
10
Energy (Mev)
1/E³
1/E²
1/E

FIG. 14

ed with a 6 c.c. counter showed a more rapid decrease with energy and closer agreement with the calculated energy dependence. The photo-fraction was determined by simply calculating the ratio of the photo peak area to the total spectra. The ratio was then plotted as a function of energy and is shown in Figure (18) . Since energies below the pair threshold were investigated Compton and photo-electric interactions only need to be considered. Letting σ_p and σ_c be the photo-electric and Compton cross-sections respectively, the photo-fraction should be simply

$$R = \sigma_p/(\sigma_p + \sigma_c)$$

provided that multiple events do not occur and the total energy of the primary electron is deposited within the sensitive volume of the detector. This relationship is also shown in Figure (18). It is immediately apparent that the measured photo-fraction exceeds the calculated value above 0.5 MeV. This deviation indicates the existence of multiple events. The relatively low probability for a primary photo-electric event at say 1 MeV makes this region a sensitive range in which to observe this effect. For comparison the ratio $\sigma_p/(\sigma_p + \sigma_c)$ is given together with the photo fractions for a 3 x 3 inch and a 1 x 1 inch NaI(Tℓ) crystal. The percentage deviation of the Ge(Li) detector from the theoretical value of photo-fraction is comparable to the deviation of a 1 x 1 inch NaI(Tℓ) crystal although the absolute value is considerably less. The photo fraction was found to be independent of geometry undoubtedly because of the almost complete depletion of the total volume. Counters having a smaller active-to-total volume ratio exhibit strong geometry dependence for this quantity.

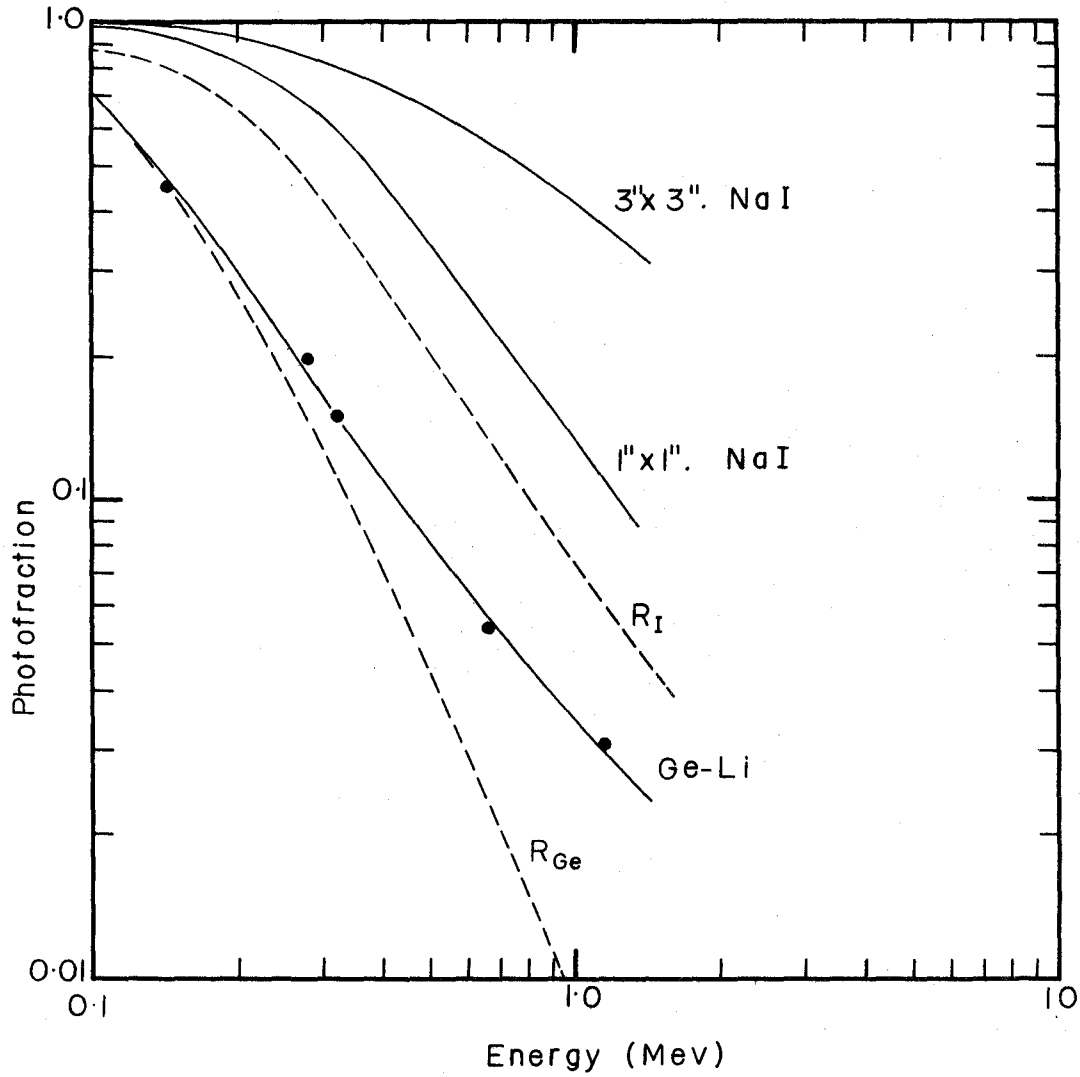
1·0
0·1
0·01
0·1
1·0
10
Photofraction
Energy (Mev)
3"x 3". NaI
1"x1". NaI
R_I
Ge-Li
R_{Ge}

FIG.18

CHAPTER V

DECAY SCHEME ANALYSIS

5.1 Introduction

The development of the Ge(Li) detector with a resolution comparable to a magnetic spectrometer and an efficiency approaching that of a small NaI(Tℓ) counter has profoundly affected the field of gamma ray spectroscopy. Two examples selected to illustrate the importance of the Ge(Li) spectrometer are presented in this work. The first involves an examination of the gamma radiation following the beta decay of the fission product Ru^{106}. The use of a Ge(Li) - NaI(Tℓ) coincidence spectrometer is demonstrated for this case. The second concerns an examination of neutron capture gamma rays emitted in the reaction $Ho^{165}(n,\gamma)Ho^{166}$. Here the efficiency and resolution of the Ge(Li) counter are utilized to investigate the complex level structure of an odd-odd nuclide.

5.2 Pd^{106} - Gamma Decay

The fission product Ru^{106} beta decays, with a one year half-life, to the ground state of 30-sec Rh^{106}. The Rh^{106} decays through one of several beta branches to excited states of Pd^{106}. The only gamma rays observed are those associated with the levels in Pd^{106}. The most definitive work on this nuclide has been reported in the Nuclear Data Sheets[12].

A Rh^{106} source was examined using a 4 mm deep x 2 high coaxial device. Initially a one dimensional run was made of all the gamma

transitions involved. The output of the counter was fed to a Tennelec 100C - TC200 preamplifier-amplifier system. The pulse height analysis was achieved using a 1024 channel Nuclear Data analyzer. These singles spectrum energies were calibrated using a Th^{232} source.

Time correlation studies were conducted to establish the decay mode of the levels in Pd^{106}. The spectrometer consisted of the Ge(Li) counter described and a 7.6 x 7.6 cm NaI(Tℓ) detector. A 90^{o} geometry was used to eliminate Compton scattering between the counters. The time markers for the coincidence circuit were generated using the standard cross-over pick-off gates described by Chase[9]. A resolving time of 2τ = 60 nsec. was employed. The pulse height information was analyzed and stored in a two parameter 4096 channel Nuclear Data N. D.-160 analyzer.

5.3 Data Analysis in Coincidence Experiment

The analyzer memory in the above experiment was divided into a rectangular array with 16 channels in the Y-dimension which were arranged to span the pulse height spectrum from the NaI(Tℓ) detector and which correspond to the 513 and 624 keV transitions. The X-dimension covered 256 channels and pulses from the Ge(Li) detector were fed into these channels. Thus in the above array there are 16 x 256 = 4096 available channels for storage of counts. When a pulse in the X-dimension, for instance in channel 100, is in coincidence with a pulse in the Y-dimension, say channel 5, a count is placed in the array at the channel position (100,5). Thus when the coincidence is extremely strong between two gamma rays, many counts will be fed into a certain position on the array and a plot of the output data can give this in-

formation. The total data will form a three dimensional surface where the Z-dimension is the number of counts in the channel and peaks will form at coordinates corresponding to strongly coincident events. However it is not necessary to plot the full surface in order to find these peaks. Assume there was a peak, or gamma ray, on the total singles spectrum, centred at channel 100 in the X-dimension. To find whether a gamma ray in the low energy spectrum in the Y-dimension was in coincidence with this peak, one simply plots the data along the Y-dimension, for the X-dimension channel 100 and subtracts from this spectrum a similar plot of the Y-dimension, for an X-channel on the continuum close to channel 100. This subtraction insures that the contributions to the true coincidence spectrum from chance events and from Compton events are eliminated.

5.4 Results

The Pd^{106} isotope singles spectrum energies and relative intensities are listed in Table II. The coincidence experiment showed that the 1132 keV, the 880 keV and the 1563 keV gamma rays populated the first excited state (513 keV). The 1053 keV transition was found to be in coincidence with the 624 keV gamma ray which in turn was in coincidence with the 513 keV gamma ray. All this information has been put in the tentative decay scheme of Figure (15). Excited states at 1082 keV, 1393 keV, 1645 keV, 2076 keV, 2190 keV, 2320 keV, 2394 keV, 2550 keV, 2575 keV, 2669 keV, 2713 keV, and 2917 keV which do not appear in the Nuclear Data sheets have been fitted to this scheme. This analysis is not an exhaustive study of the Pd^{106} gamma decay but purely aids in showing that Ge(Li) detectors are useful tools in the further decay studies of relatively well known nuclides.

TABLE II

Decay of Pd^{106}

Observed γ-Rays (keV)	Corrected Relative Intensity
513	5.9
624	1.6
880	1.1
1050	0.69
1082	0.18
1132	1.1
1170	0.54
1195	0.14
1498	0.09
1563	0.45
1770	0.06
1802	0.06
1931	0.03
1993	0.06
2118	0.08
2320	0.03
2373	0.06
2400	0.01
2410	0.04
2445	0.01
2550	0.01
2575	0.005
2669	0.002
2713	0.01
2917	0.0001
3035	0.0003

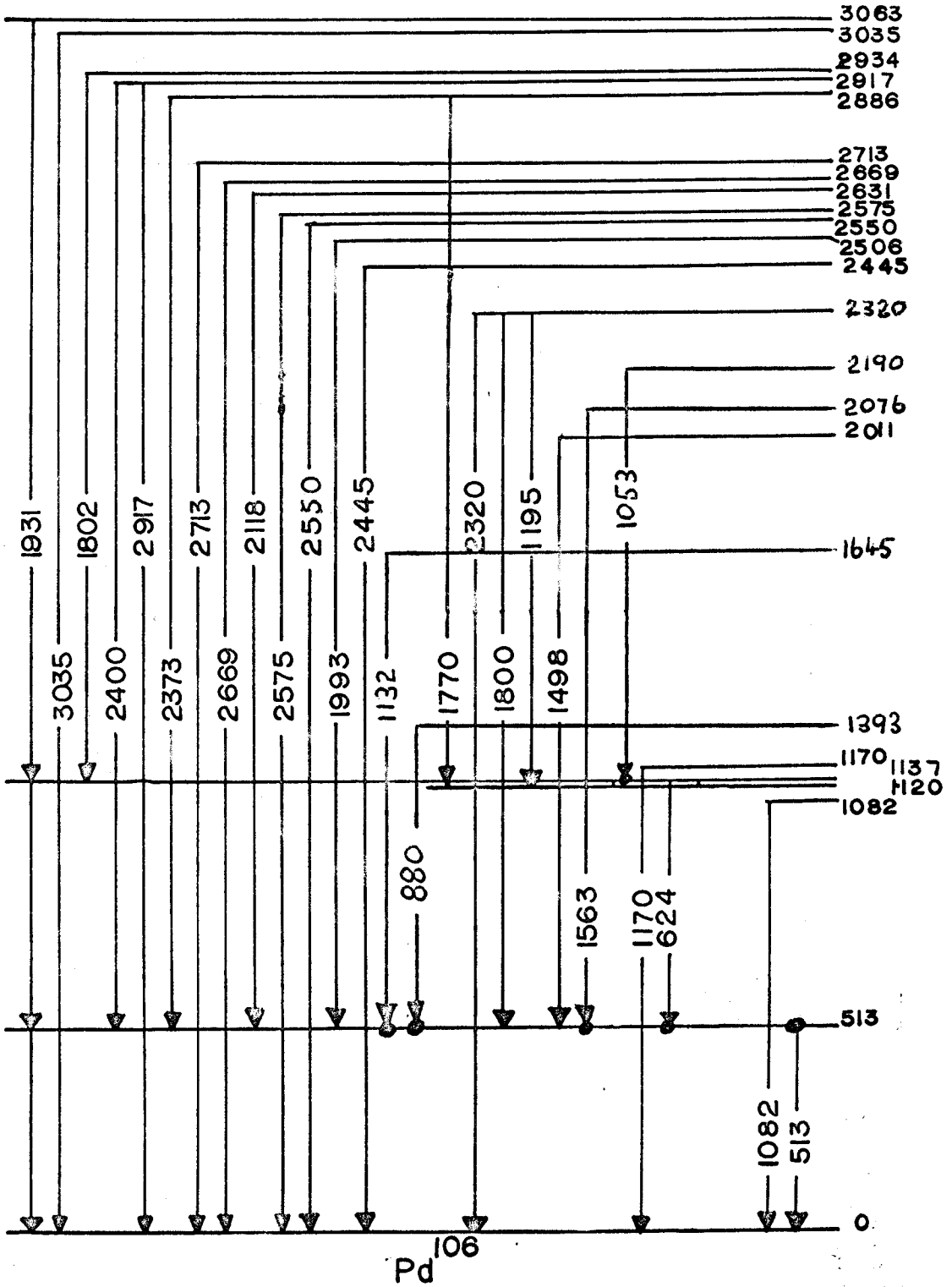
3063
3035
2934
2917
2886
2713
2669
2631
2575
2550
2506
2445
2320
2190
2076
2011
1645
1393
1170
1137
1120
1082
513
0
1931
3035
1802
2400
2917
2373
2713
2669
2118
2575
2550
1993
2445
1132
880
2320
1770
1195
1800
1053
1498
1563
1170
624
1082
513
106
Pd

FIG. 15

5.5 $Ho^{165}(n,\gamma)Ho^{166}$ - Neutron Capture Gamma Decay

The thermal neutron capture in Ho^{165} was experimentally performed in the McMaster Nuclear reactor using a vertical through tube facility situated adjacent to the reactor core. Neutrons were deflected up the tube by a 5 kg graphite scatterer and collimated by annuli of boron carbide, paraffin and lead. This apparatus resulted in a thermal neutron beam 2 cm in diameter and 10^7 n/sec. A sample of high purity holmium oxide weighing approximately 2 gms was placed in the tube at the level of the reactor bridge and the detector was placed adjacent to the sample outside the tube. Scattered neutrons were absorbed by a tube of lucite and Li^6F surrounding the sample.

Because of the high level density characteristic of the odd-odd rare earth nuclides two sets of single parameter runs were necessary. The first investigated the energies from 0 to 1 MeV and to calibrate this run the gamma rays following the beta decay of Mn^{54}, Eu^{152} and Eu^{154} were used. The second involved the energies from 4 to 7 MeV. The calibration of the high energy end was accomplished by analyzing a mixture of Ho^{165} + Cl^{35} and using the accurately known energies of the intense chlorine lines on the spectrum to calculate the energies of intense peaks of the holmium gamma rays. The Ho^{165} sample alone was put in the beam and the spectrum was analyzed and the energies of the weaker lines were calculated.

The detector used to analyze the data was a 6 cm^3 Ge(Li) detector and its efficiency curve was similar to that shown in Figure (14) except for the fact that it did not exhibit multiple event collection to the same degree the 10 cm^3 counter efficiency curve did. The low

energy photo-efficiency of the 6 cm^3 counter exhibited a $E^{-1.8}$ form[5] where E is the energy of the observed gamma ray.

5.6 Results

Some of the high and low energy gamma rays observed in the experiment are listed in Table III along with those observed by Groshev and Motz[13]. Energy and corrected intensity criteria were used to deduce the tentative decay scheme shown in Figure (16). The high energy gamma rays observed in this work interact in the counter primarily by producing positron-electron pairs but some photo-electric events will also occur. The germanium cross-section curves of Figure (9) show the relationship. When the pair is produced the electron will lose its energy to the counter but the positron loses its kinetic energy and then annihilates with an electron forming two 511 keV gamma rays. One or both of these secondary gamma rays may escape from the counter and from the spectrum in Figure (17) it can be seen that the 2nd escape i.e. both gamma rays escape peaks are much more intense than the 1st escape peaks or the photo peaks. Thus to calculate the energies of the gamma rays, only 2nd escape peaks should be used and this involves eliminating 1st escape peaks and photo peaks. This has been done in analyzing the Ho^{166} decay and all energies have been corrected to the full energy of the interacting gamma ray. The neutron separation energy found for this reaction is 6.248 MeV and agrees well with the energy of 6.243 MeV quoted by Motz[13]

TABLE III

$Ho^{165}(n,\gamma)Ho^{166}$

Gamma Ray Number	Observed γ-Rays (MeV)	Relative Intensity	Groshev et al[14] Observed γ-Rays (MeV)	Intensity*
48	6.105 (6)	0.25	6.105 (7)	0.02
			6.079 (7)	0.04
47	6.049 (6)	0.63	6.057 (5)	0.33
45	5.976 (6)	0.20	5.987 (6)	0.09
			5.966 (8)	0.03
			5.917 (8)	0.02
43	5.864 (6)	0.58	5.872 (5)	0.29
42	5.806 (6)	0.80	5.813 (5)	0.76
41	5.758 (6)	0.50	5.766 (5)	0.34
			5.729 (8)	0.03
			5.699 (8)	0.04
39	5.676 (6)	0.41	5.688 (5)	0.19
38	5.638 (6)	0.29	5.652 (5)	0.13
			5.612 (6)	0.06
37	5.571 (6)	0.22	5.583 (6)	0.10
			5.552 (7)	0.03
36	5.538 (6)	0.11	5.529 (7)	0.13
35	5.513 (6)	0.23	5.520 (7)	0.13
			5.489 (7)	0.06
34	5.415 (6)	0.68	5.437 (6)	0.33
			5.420 (7)	0.09
33	5.342 (6)	0.25	5.366 (7)	0.17

* Photons per 100 neutron captures

TABLE III (continued)

$Ho^{165}(n,\gamma)Ho^{166}$

Gamma Ray Number	Observed γ-Rays (MeV)	Relative Intensity	Groshev et al[14] Observed γ-Rays (MeV)	Intensity*
32	5.323 (6)	0.30	5.298 (7)	0.05
			5.242 (7)	0.10
30	5.196 (6)	0.56	5.215 (5)	0.33
			5.180 (5)	0.33
29	5.163 (6)	0.60	5.150 (8)	0.04
			5.125 (6)	0.26
28	5.106 (6)	0.37	5.104 (7)	0.06
27	5.083 (b)	0.25	5.082 (5)	0.30
25	5.029 (6)	0.09	5.011 (7)	0.12
24	4.979 (6)	0.22	4.999 (6)	0.26
23	4.953 (6)	0.17	4.941 (5)	0.36
22	4.908 (6)	0.94	4.897 (7)	0.12
			4.882 (7)	0.12
21	4.869 (6)	0.17	4.857 (5)	0.39
			4.824 (5)	0.14

Observed γ-Rays (keV)	Relative Intensity	Motz et al Observed γ-Rays (keV)
115.6 (1.0)	0.38	
135.4 (1.0)	1.00	
147.5 (1.0)	0.14	
179.5 (1.0)	0.23	169.3 (3)
195.9 (1.0)	0.14	190.9 (7)
219.8 (1.0)	0.24	
237.6 (1.0)	0.27	

* Photons per 100 neutron captures.

TABLE III (continued)

$Ho^{165}(n,\gamma)Ho^{166}$

Observed γ-Rays (keV)	Relative Intensity	Motz et al Observed γ-Rays (keV)
288.3 (1.0)	0.24	263.3 (1)
303.5 (1.0)	0.19	
332.2 (1.0)	0.15	340.
370.9 (1.0)	0.17	
390.0 (1.0)	0.17	372.9 (5)
400.5 (1.0)	0.35	
410.1 (1.0)	0.46	
425.3 (1.0)	0.98	430.4 (5)
455.8 (1.0)	0.11	
488.5 (1.0)	0.17	477.7 (2)
543.6 (1.0)	0.37	
		535 (4)
		555.5 (2)
		594.4 (1)
634.2 (1.0)	0.04	636.0 (2)
659.2 (1.0)	0.07	663.0 (2)
		690.3 (2)
736.5 (1.0)	0.06	718.8 (1)
		770 (3)
		816.1 (6)
885.4 (1.0)	0.05	881.4 (15)

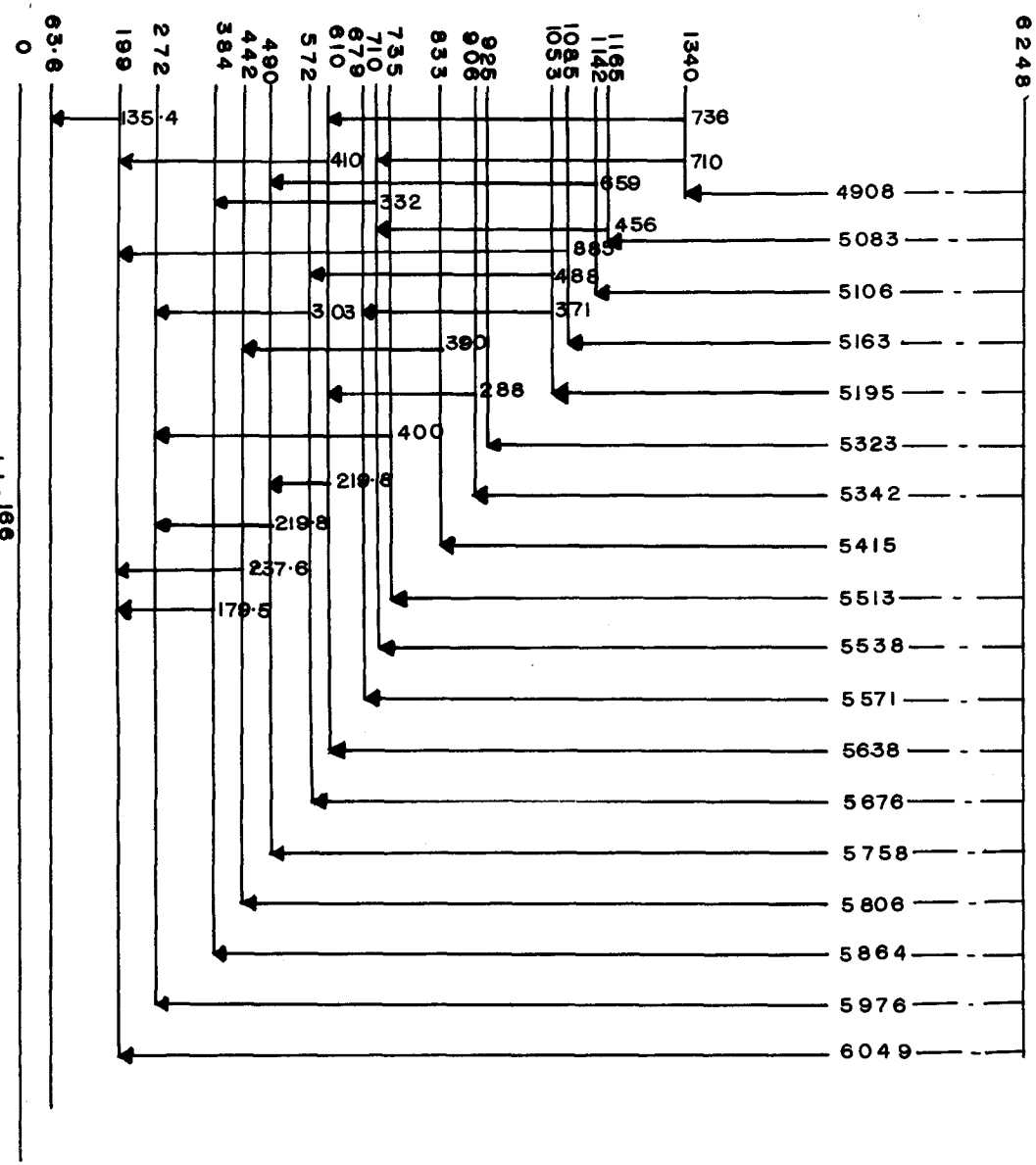
Ho 166
0
63·6
199
272
384
442
490
572
610
679
710
735
833
908
925
1053
1085
1142
1165
1340
6248
135·4
736
410
710
659
4908
332
456
5083
885
488
5106
303
371
5163
390
5195
286
400
5323
219·6
5342
219·8
5415
237·6
5513
179·5
5538
5571
5638
5676
5758
5806
5864
5976
6049

FIG. 16

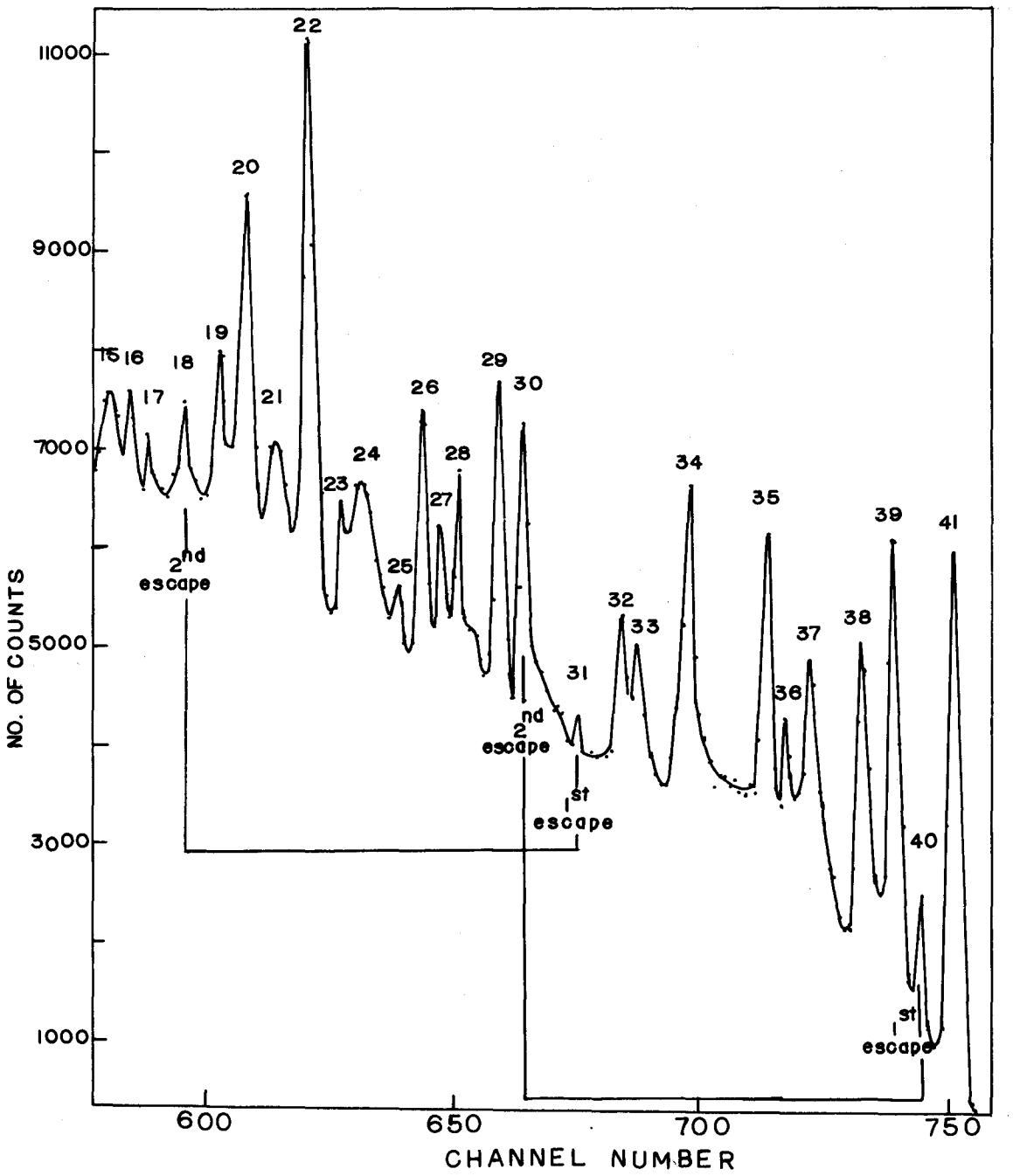
11000
9000
7000
5000
3000
1000
NO. OF COUNTS
600
650
700
750
CHANNEL NUMBER
15
16
16
17
18
19
20
21
22
23
24
25
26
27
28
29
30
31
32
33
34
35
36
37
38
39
40
41
2nd escape
2nd escape
1st escape
1st escape

FIG. 17

REFERENCES

(1) F.A. Lehrer and H. Reiss, Journal of Applied Physics 33, 2353-2359 (1962).

(2) F. J. Morin and H. Reiss, Journal of Physics and Chemistry of Solids 3, 146-209, (1957).

(3) H. L. Malm, A. J. Tavendale, and I. L. Fowler, Canadian Journal of Physics, 43, 1173 (1965).

(4) G. Armantrout, I.E.E.E. Transactions on Nuclear Science N.S. 13, 84 (1966).

(5) H. J. Fiedler, L. B. Hughes, T. J. Kennett, W. V. Prestwich and B. J. Wall, Nuclear Instruments and Methods, 40, No. 2 (1966).

(6) D. A. McKay. Thesis: Lithium-Drifted Gamma Radiation Detectors, McMaster (1964).

(7) A. J.Tavendale, I.E.E.E. Transactions on Nuclear Science, N. S. 12, 1, 255 (1965).

(8) H. L. Malm, C.R. G.R. - 1236, Chalk River (1966).

(9) R. L. Chase, Nuclear Pulse Spectrometry. McGraw-Hill, (1961).

(10) R. L. Heath, A.E.C. Research and Development Report, I.D.O.-16408. (1957).

(11) E. Storm, E. Gilbert, H. Israel, A.E.C.-report LA-2237 (1958).

(12) Nuclear Data Sheets A = 106, N.R.C. 60-4-43 (1961).

(13) Nuclear Data Sheets A=166, Vol. 6, Set 4, (1965).

(14) L. V.Groshev, N. Sladiev, Kurelatov Institute of Atomic Energy Report IAE - 719 (1964).

(15) E. M. Pell, J. Appl. Phys., 31, 291 (1960).

(16) G. L. Miller, B. D. Pate and S. Wagner, I.E.E.E. Trans Nuc. Sci. NS-10, 220 (1963).

(17) The I.E.E.E. Transactions on Nuclear Science, Vol. NS-13, 1, Feb. (1966).